2019

A Critical Analysis of the Wind Generated Effect on the Rate of Overtopping on the Hinkley Point C Sea Wall Through the use of Physical Modelling

Alberto, I.

Alberto, I. (2019) 'A Critical Analysis of the Wind Generated Effect on the Rate of Overtopping on the Hinkley Point C Sea Wall Through the use of Physical Modelling', The Plymouth Student Scientist, 12(1), p. 135-186.
http://hdl.handle.net/10026.1/14685

The Plymouth Student Scientist
University of Plymouth

*The Plymouth Student Scientist, 2019, **12**, (1), 135-186*

A Critical Analysis of the Wind Generated Effect on the Rate of Overtopping on the Hinkley Point C Sea Wall Through the use of Physical Modelling

Ian Alberto

Project Advisor: Dr Martyn Hann, School of Engineering, Plymouth University, Drake Circus, Plymouth, PL4 8AA

Abstract

It is widely observed that storms and the associated extremes of wind and wave conditions result in dramatic cases of sea defence overtopping. This phenomenon highlights a gap in knowledge that the industry standard EurOtop method for calculating overtopping volumes does not account for the effect of wind. This study aims to outline a generalised relationship between increasing onshore wind speed during storm events and the resulting volume of sea defence overtopping coupled with spatial distribution of the overtopped water. With design criteria being site-specific, this physical model experiment will recreate the conditions at Hinkley Point C to determine what extent the seawall has been designed and constructed to cope with these climatic and meteorological effects. Three water levels will be tested to identify overtopping rates and to establish the extent of hazard zones behind the coastal structure. This paper provides evidence that there is a strong exponential relationship between onshore wind speed and an increase in overtopping volume. The effect of wind increases the overtopping rate by up to 20 times at scale than that of no onshore wind. This effect of wind is a critical factor in design but not well researched within the industry.

With this construction project at the central hub of the industry's scrutiny, the necessity to understand and quantify the effects of overtopping due to the associated dangers is crucial.

Introduction

Context

In recent years, rising sea levels have been a principle concern to the population and with the United Kingdom (UK) having a high coast/area ratio, natural processes like erosion, flooding and land loss are becoming more prominent and imposing detrimental impacts on coastal areas. With 21% of the world's population living within 30km of the coast (Gommes et al., 1997) and these populations growing at twice the global average (Bijlsma et al., 1996), the development and utilisation of coastal zones have greatly increased with coasts undergoing large socio-economic, environmental and physical changes due to their desirable sceneries and necessity.

Seawalls are a common form of coastal defence, protecting coastlines against erosion, extreme water levels and flooding caused by combinations of high tides, waves, wind set-up and storm surges driven by low-pressure systems (Jones, Zou and Reeve, 2011). Seawalls reduce but not wholly prevent overtopping and are designed to provide levels of protection given by acceptable mean overtopping discharges at given return periods (Allsop et al., 2005). With sea level predicted to rise by 0.34m by 2100 (Church and White, 2006) and with storms becoming significantly rougher in the form of stronger and more frequent waves, flooding is more likely to occur in unprepared and vulnerable areas consequently leading to failure, in terms of performance (Geeraerts et al., 2006). Hence, it is imperative that these structures are well understood in terms of their buildability, failure mechanisms and primary purpose.

Wave overtopping is the critical response of most sea defence structures. It is the phenomenon by which a volume of water passes over the crest of a coastal structure per unit of time. Overtopping is caused by wave run-up, wave splash or wave spray and is significant as it can be dangerous to vehicles and pedestrians leading to the damage of structures on the leeward side in the form of obstruction and erosion.

Hinkley Point C (HPC) is a Nuclear Power station, amidst construction, located in Somerset, England. With the power station aiming to deliver 7% of electricity when other nuclear power stations will have closed down (National Audit Office, 2017), HPC is of high importance and longevity. The seawall not only prevents extensive erosion of the cliff face but provides protection for the public footpath; its importance is of particular value and with the Nuclear Power station having a design life of 100 years, the seawall must be durable for a minimum of this time.

Aims and Objectives

This experiment aims to identify how the rate of overtopping and spatial distribution of overtopped water landward side of the seawall is influenced by onshore wind and to what extent the wall has been designed to cope with wind and varying water levels.

Physical modelling can be used to examine the behaviour of a structure under a set of specified conditions. With this knowledge, a scaled down cross-section of the wall was constructed and tested based on the Froude scaling laws. The physical model exists so that the major dominant forces acting in the prototype system are reproduced in the model according to the laws of similitude.

Specifically, the key objectives of this research are to:

1. Design, construct and test a physical model of the Hinkley Point C seawall with wind-assisted overtopping using the COAST laboratory
2. Outline key relationships that have been observed in terms of overtopping, wind speed and spatial distribution
3. Identify to what extent the Hinkley Point C seawall has been designed to cope with a 1 in 1, 1 in 100 and 1 in 1000 water level.

Value of this research

There are currently equations and formulae to accurately predict mean overtopping volumes at vertical seawalls however further research is warranted on discharge distances to ameliorate safety behind seawalls.

With a lack of published research and limited data existing on this site and the combined effect of wind-generated overtopping and spatial distribution of coastal structures (Allsop et al., 2005; Wolters and R.A. van Gent, 2007), it is hoped that the resulting conclusions will be applicable to the wider industry thus leading to the development of industry standards such as EurOtop (2016). With a lack of sufficient information on wind related overtopping, this experiment aims to provide an insight and conclusion as to whether the Hinkley Point C sea wall has been designed to limit the extents of overtopping within this stochastic environment, and if not, to what magnitude it occurs.

Review of previous wind related overtopping

Introduction to Literature review

Breaching of the coastline can lead to significant damage and hence the need to fully understand the mechanisms of failure to coastal structures is critical. Current coastal defence schemes are under an ever-increasing threat from environmental and anthropogenic pressures.

A key performance failure mechanism for seawalls is the phenomenon of overtopping. Within this project, context is provided relating to the coastal processes and types of waves that lead to overtopping before investigating the relevant climatic and meteorological effects, associated overtopping hazards and various effects arising with physical modelling. Hard and soft engineering coastal defence structures are mentioned before introducing the necessity of the coastal defence scheme used at Hinkley Point C. Importance is also appreciated with regards to informing design decisions.

Coastlines

A coastline is *a transient and continually changing strip of land that borders the sea along a continent or island* (Nationalgeographic.com, 2017). The surrounding waves sculpt the coastline through swash (upward rush of water that deposits sediment) and backwash (carries sediment back out to sea). This continuous transportation of sediment through wave activity accelerated by offshore wind can be classified as longshore and cross-shore drift and are the leading processes responsible for shaping the coastline. These changes in profile have a great deal of effect on the socio-economic stability in an area hence the need to protect and preserve the coastline from physical and anthropogenic land loss.

At Hinkley Point C, it is a necessity for this power station to be located along the coastline mainly for water cooling effects and for steam generation that powers the turbine, in turn producing electricity. In this circumstance, the need to preserve infrastructure is a priority and hence the need for an effective coastal defence.

Hard and Soft engineering

The majority of the UK's coastline is preserved and maintained in an attempt to reduce the impacts of coastal erosion. Coastal defences generally fall into two varying categories, "hard" and "soft" engineering. Soft engineering methods are more environmentally friendly and usually a cheaper approach. These methods work in conjunction with natural processes to protect the shoreline against the dynamic nature of this environment. Hard engineering can be costlier and a more intrusive alternative however provides a more robust and conservative system and most importantly, minimises risk. Elements of both hard and soft engineering should be used in unification to provide an optimal coastal defence scheme to coincide with the invasive nature of the coastal system.

Sea Walls

Seawalls, an example of hard engineering, are a form of a coastal defence used to minimise the effects of coastal erosion along coastlines. They are made of stone and concrete and built to withstand forces imposed by breaking waves and dissipate or absorb wave energy depending on design (Bird, 1996). These structures are required in environments when waves reach the coast with too much energy causing damage through flooding and erosion. Seawalls preserve private structures and protect the public however accelerate passive erosion in front of the wall in the form of scour by concentrating the energy rather than dispersing it along the stretch of the coast. Scour produces a drop in beach level and over many years, the seawall can undermine and eventually collapse (French, 2004). This risk can however be reduced when using rock armour at the toe to dissipate the energy from the waves or sheet pile foundations – 2 methods adopted within the HPC design brief.

There are varying designs of seawalls commonly used based on the surrounding conditions; curved, stepped and vertical. Vertical seawalls are highly reflective which results in rapid lowering of the beach ((www.geodata.soton.ac.uk), 2007). However, these seawalls are most commonly used simply due to practicality and effectiveness of the structure in regards to construction and purpose. The depth of water and angle

of slope fronting a seawall governs the wave action exerted on the wall and therefore, prior to construction, research on water levels are needed for hydraulic behaviour and economic assessment.

Rock armour

Rock armour is usually lined at the toe of shoreline structures to protect them against scour or erosion. These boulders absorb the wave energy due to their high permeability which is then dispersed through the rocks and refracted back out to sea. When constructing the arrangements of these rock armour layers, contractors ensure the boulders are packed tightly together in an attempt to produce a more stable structure and minimise voids that may present health and safety hazards (CIRIA, 2007). The main limitation of rock armour are cost e.g. transportation costs of barge and excavator. Figure 1 shows the rock armour used at HPC.

Overtopping

Overtopping is defined *as the amount of water flowing over the crest of a coastal structure* due to wave action per unit of time (Geeraerts et al., 2006). It occurs when wave run-up exceeds the structure freeboard. Seawalls can fail either in performance or it's holistic structural ability and overtopping and scour are examples of these respectively.

Figure 1: Rock armour placed at Hinkley Point C prior to construction

The principal equation used to calculate mean overtopping discharge is:

$$\frac{q}{\sqrt{gH_{m0}^3}} = 0.0014\left(\frac{H_{m0}}{hs_{m-1,0}}\right)^{0.5}\left(\frac{R_c}{H_{m0}}\right)^{-3} \qquad \text{valid for } R_c/H_{m0} \geq 1.35 \qquad (1)$$

H_{m0} – significant wave height from spectral analysis (m) **R_c –** crest freeboard (m)

q – overtopping discharge (m^3/s) per m **g** – gravity (m/s^2)

There are 3 types of overtopping that occur; “green water” overtopping where a continuous sheet of water passes over the crest, “splash” overtopping that occurs when waves break on the seaward side of the structure to produce significant volumes of splash that are carried over by either their own momentum or onshore wind and lastly “spray” overtopping which is produced by the interaction between wind and waves causing water to be carried over the structure in the form of spray (EurOtop, 2016).

Contributory factors to overtopping

The above overtopping types are amplified by the following component that increases the likelihood of overtopping. This component is an aspect that must be considered during design.

Mean sea level

Changing sea level is a principal detriment of shoreline position and coastal landforms (Phillips and Crisp, 2010). This issue is multifaceted and produces a range of environmental problems. Prediction of water levels are deemed necessary for wave run-up or wave overtopping, 2 factors often taken into consideration during design of the essential crest level of a coastal structure.

Mean sea level can be raised in four fundamentally different ways:

1. **Thermal expansion** - altering the volume of the ocean mass by warming.
2. **Adding water mass** which primarily comes from melting land ice i.e. glaciers.
3. **Change in depths** of ocean basins by movement of the Earth's crust.
4. **Isostatic rebound** – relative water level change due to the readjustment of a land mass which was once subjected to a large load.

Research conducted by Phillips and Crisp (2010) using tidal gauges, observed that an increase of 150mm-185mm is expected by 2100 specifically at HPC. With an increase in sea level, there is an even bigger need to ensure coastal structures are designed to limit overtopping especially in the case of HPC.

Parameters affecting overtopping

Below outlines critical parameters that affects overtopping and are taken into account when designing coastal structures.

Wave height

Wave height is defined as the vertical distance measured from the crest and trough (Iglesias, 2017). The most commonly used parameter is the significant wave height, which is the average height of the highest one-third of waves and denoted by the notation H_S or $H_{1/3}$.

Wave period

Wave period is the time for two successive wave crests to pass a given measuring point and is given the notation T (Iglesias, 2017). The most commonly used wave periods are peak period, T_p.

Wave steepness

Wave steepness is defined as the ratio of wave height to wavelength

$$s_0 = H_{m0}/L_0 \qquad (2)$$

and is a dimensionless parameter. A steepness of $s_0 = 0.01$ indicates a typical swell sea and a steepness of $s_0 = 0.04$ to 0.06 a typical wind sea (EurOtop, 2016).

Foreshore

The foreshore refers to the region in front of a coastal structure and as the foreshore transitions from deep, to shallow, to very shallow, wave breaking is induced with a decrease in depth. In general, the transition between shallow and very shallow foreshores can be assumed as the point where the incident wave height has decreased by approximately 50% or more as a result of breaking (EurOtop, 2016).

Crest freeboard

The crest height of a structure, relative to the still water level (SWL) is defined as the crest freeboard, R_c, and the armour freeboard, A_c, being the height of the horizontal part of the crest, measured relative to SWL as seen in figure 2 (EurOtop, 2016). Waves at vertical walls may give rise to up-rushing water induced by impulsive wave breaking or presence of rock armour that could overtop over the crest.

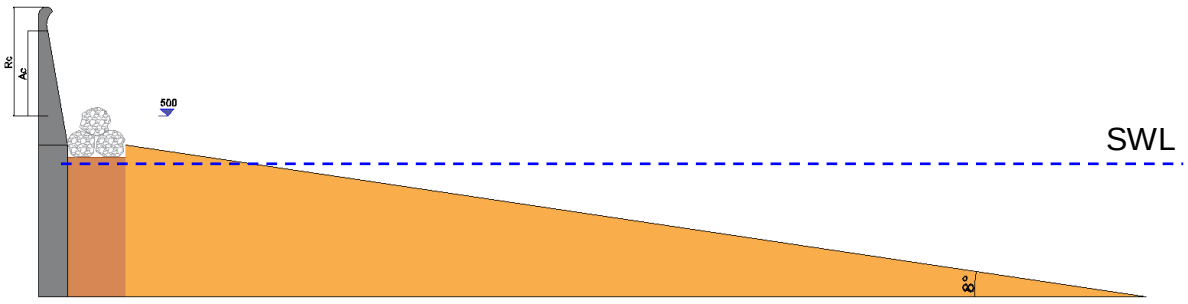

Figure 2: Cross section of Hinkley Point C seawall showing the freeboard

Wave return

To decrease overtopping water, a wave return is designed and situated on top of the structure to deflect the up-rushing wave. These can be pre-cast or fixed in-situ with vertical dowels.

Spatial Distribution and Throw Speed

Throw speed is defined as the vertical speed at which the overtopping stream of water leaves the crest of the structure. Spatial distribution is the distance and direction of the overtopped discharge. Wind modifies the physical form of the overtopping volume in terms of break-up, altering the speed and direction of overtopped water (EurOtop, 2016).

Measuring Overtopping

Overtopping is often expressed in terms of q with two main methods to measure overtopping discharge. The most common method is to record the total volume transmitted over the structure during a set period of time or waves depending on whether regular or irregular waves are being tested (Pullen, 2009). This is measured per meter per second ($m^3/m/s$) and can be used to determine a design overtopping discharge rate and multiplied by 1000 to convert the discharge into litres (Pullen et al., 2003). The second considers the maximum volume per overtopping wave. This method is predominantly used for analysing situations where a large volume of water could have a destructive impact.

Overtopping Hazards

Urban infrastructure located along coastlines are protected against wave overtopping and further erosion through the use of well-designed coastal structures. These structures limit overtopping volumes rather than eliminate it fully especially under storm action where waves overtop these structures frequently and violently.

EurOtop (2016) states that existing sea defences in the UK have offered protection far lower than what is expected and this is apparent from the UK floods of 2014 that caused a lot of damage to property behind seawalls. Allsop (2008) mentions that new developments should provide protection up to a 1 in 200 year event which is equivalent to an annual probability of 0.005% especially with external factors such as climate change that increases the frequency and intensity of storm events. HPC does not follow this criterion.

Vertical wall structures experience a greater deal of impulsive breaking which results in more violent overtopping with greater speeds. By improving the knowledge and understanding on hazards in areas affected by overtopping, the analysis of hazard zones and effects of wind will be more familiar thus allowing engineers to identify vulnerable infrastructure and hazardous areas (Bruce et al., 2005).

Climatic and Meteorological Effects on Overtopping

Shorelines have not reached a dynamic equilibrium and are still adjusting in orientation. Areas in the UK are still in a transgressive phase where they are in a period of rising relative sea level (Reeve, Chadwick and Fleming, 2012)

Problems for coastal engineers occur in regards to management when natural climatic processes start to impinge on human activity. To fully appreciate the effect that the wider environment has on the coast, 4 influential elements are discussed.

Tides

Around the UK, the largest fluctuations behind tidal movements are driven by astronomical tides which are a result of the periodic rotation of the sun and the moon around the earth each day which enables for the accurate prediction of tidal levels. The gravitational effect over the surface of the ocean creates tides with distinct periods, categorised as diurnal and semi-diurnal.

In the UK, semi-diurnal tides are mostly experienced meaning there are two high tides and two low tides each day that are roughly spaced every 12hour 25min (Metoffice.gov.uk, 2017). The Bristol Channel exhibits a tidal range (the vertical difference between high and low water) that categorises it as the second highest semi-diurnal range in the world with a mean spring range of 12.2m and a mean neap range of 6.0m (Neill et al., 2009).

The Bristol Channel experiences a high tidal range caused by the shape and contour of the coast and the surrounding ocean, which creates an even bigger need for a safe coastal design. With the Bristol Channel being funnel shaped and this area passing through the tidal bulges twice a day due to the Earth's rotation, the surrounding water is compressed causing it to increase in range and rate. Van Rijn (2018) further mentions that this effect of funnelling affects the tidal propagation caused by the decrease of the channel cross-section through damping caused by bottom friction, reflection from boundaries and by deformation due to differences in propagation velocities. Secondly, the greater the mass of water that influences the area, the greater the tidal range. With the Atlantic Ocean directly west of the Bristol Channel, the tidal range similarly increases. Lastly, the mountains and high ground that lie directly north and south of the Bristol Channel respectively, create this aforementioned effect of funnelling from the prevailing South-Westerly wind and thus increasing the velocity and accelerating the tidal range within this area (ThoughCo.com, 2017). The wedge-shaped topography concentrates the energy density and the large tidal range at the mouth is converted into an extremely large tidal range at the head of the estuary (Neill et al., 2009).

Bathymetry is the portrayal of the ground surface below water. Tides consist of long waves so the phenomena of refraction and shoaling can lead to considerable amplification of tidal levels in shallow seas.

Springs and Neaps

The Moon and Sun are at their greatest effect when in line with the Earth and have their lowest effect when at right angles to each other. After a full Moon, a locality experiences its highest high waters and lowest low waters, and the tides in this period are categorised as Spring Tides. Similarly, during the first and last quarters of the Moon, the lowest high waters and the highest low waters of the month are experienced, and these are known as Neap Tides (Visitmyharbour.com, 2017).

Wind Effects

Wind is produced from pressure differentials travelling from high to low pressure. The Admiral Tide Tables (ATT) are used to give daily predictions of the times and heights of high and low waters for standard and secondary ports.

When water molecules receive energy from the wind, they move forward slightly forming a circular pattern. With the waves progressing to the coastline, the depth decreases and the diameter of these circular patterns decrease causing the patterns to become elliptical. The waves grow in height and steepness and leads to depth induced breaking (ThoughtCo, 2017). Wind affects overtopping processes through changing the shape of the incident wave crest resulting in altering the wave interaction at the wall, blowing up-rushing water over the crest of the structure and through modification of the physical form of the overtopping volume. This breaking and modification that occurs determines the type and volume of overtopping experienced by the structure.

With the location of this seawall along an exposed coastline, there is a great need in understanding and predicting how the wind reacts in this coastal environment.

Surges

Storm surges are caused by a rise in coastal waters above the astronomical high tide generated by a passing storm. The atmosphere acts upon the sea in two noticeably different ways; a reduction in the atmospheric pressure induces a dome of water causing the seawater to rise or an increase in atmospheric pressure which will produce a decrease in sea level. The Bristol Channel is affected by storm surges which are generated by the passage of Atlantic depressions across the UK. Meteorologically, a storm surge will induce higher energy waves and produce correspondingly greater changes than a period of atmospheric calm (French, 2004).

In order to predict extreme water levels, long-term analysis of water level data is required however if a lack of research is available, it may be necessary to predict surge levels using theoretical equations. A resultant tidal curve can be produced that combines astronomical tide with a storm surge that defines the increase and decline of surge over time (Environment Agency, 2011).

Return Periods

Gōda (2010) defines return periods (T_R) as *the average duration of time during which extreme events exceed a certain threshold value once*. Coastal structures are designed to provide protection given by a tolerable mean overtopping discharge at given return periods set by national regulations or guidelines.

$$\text{Probability of exceedance (X)} = \frac{1}{T_R} \qquad (3)$$

By utilizing statistical models, return levels can be quantified to determine extreme significant wave heights used as a design criterion for long lasting coastal defences,

but also scaled to replicate wave conditions during physical modelling (Sartini, Mentaschi and Besio, 2015).

Joint Probability

HR Wallingford (2000) defines joint probability *as a combination of multiple partially related environmental factors that happen simultaneously*. Large storms with high waves and water levels can coincide with spring tides to inflict damage to sea defences and the need to consider the joint probability of these factors when assessing design conditions for coastal structures is required. The assumption of dependence leads to a very conservative design but conversely the assumption of independence can lead to an under-designed defence.

Coastal Defence Structure Design Criteria

This section outlines further criteria beyond those previously discussed that must be considered when designing any coastal structure.

Incident Wave conditions

Incident wave conditions are one of the main primary factors to be considered when designing sea walls. To assess the overtopping at vertical structures, the interaction between waves and the structure must be identified as different interactions produce different results in terms of overtopping discharge.

From deep water to the shoreline, waves are transformed by their interaction with the seabed and coastal structures. The two main wave processes impacting on vertical walls can either be breaking (impulsive) or non-breaking waves (non-impulsive). Impulsive conditions occur on vertical walls when waves are larger relative to the water depth. This shallow water depth causes an increase in wave height leading to an increased steepness causing the waves to plummet directly onto the wall with high volumes of pressure but not for long periods of time. It causes a large flume of aerated water to violently jet upwards over the seawall. Vertical wall structures are often situated at the shoreline position fronted by shallow water especially in areas of significant tidal range where waves can break directly on the structure (Bruce et al., 2005). In these conditions, some waves will break violently against the wall with forces reaching 10–50 times greater than for non-impulsive conditions (Bruce et al., 2005). This unpredictable phenomenon creates problems for engineers during design calculations however EurOtop (2007) have formulated an equation combining water depth, wave height and period to distinguish between impulsive and non-impulsive waves.

$$h* = 1.35 \frac{h}{H_{mo}} \frac{2\pi h}{g*{T_m}^2} \qquad (4)$$

Non-impulsive waves dominate when h* > 0.2; impulsive waves when h* ≤ 0.2.

During non-impulsive conditions, generally no overtopping occurs however if it does occur, the wave runs up the face of the structure and gives rise to the “green water” overtopping.

There are 3 breaking waveforms that cause shock pressure intensities greater than pressures induced by similar sized non-breaking waves: Ventilated, compression and hammer shock. These pressures on the face of the structure result in rapid, high-intensity shock pressures leading to overtopping or potential damage (Hughes, 1993). Hudson et al. (1979) further mentions that the magnitude of these shock pressures are based upon 4 physical factors: the wave characteristics (water depth at toe, foreshore slope), concentration of entrained air as the wave impacts, pressures in trapped air pockets and pressures in air cushions.

With varied differences between impulsive and non-impulsive conditions, it is necessary to determine the most dominant overtopping regime for a given structure to predict overtopping (EurOtop, 2016). This is further proved by Müller et al. (2008) who examined that a change from non-impulsive to impulsive conditions substantially increases overtopping.

Oblique Wave overtopping

The oblique wave angle (β degrees) is the angle between the propagation of waves and the line perpendicular to the structure. The coastline in this study is subjected to an oblique wave attack from waves propagating up the channel due to prevailing winds predominantly from the South-westerly direction. With the oblique nature of the waves that arrive, wave overtopping is typified by the growth of the Mach-stem wave type which grows as it propagates along the seawall. When these oblique waves are reflected from the vertical seawall with a small incident wave angle, large waves are generated to propagate along the wall resulting in an overtopping effect.

Tolerable Overtopping

Socioeconomic and safety arguments determine the allowable overtopping alongside national guidelines estimated based on the size and use of the receiving area, the extent of landward drainage and given return periods. These tolerable levels are therefore treated on a site-specific basis.

One of the primary objectives of an engineer designing coastal sea defence structures is to limit overtopping discharge to acceptable levels through the inclusion of a minimum crest height (Besley, Stewart and Allsop, 1998). At HPC, the public footpath will be limited to a maximum overtopping rate of 0.1 litres per metre per second (l/m/s) between a 1 in 1 and 1 in 100 year design event. When determining the tolerable overtopping discharge during design at HPC, a lack of consideration has been taken for the effect of wind even with this phenomenon likely to increase the overtopping discharge especially at lower volumes (De Rouck et al., 2005)

Numerical and Physical Modelling

The analysis of coastal dynamics is difficult due to the constant rate at which the coast changes and the complex interactions that occur with shoreline responses as a result of the unpredictable nature of the coastal environment (Reeve, Chadwick and Fleming, 2014). With numerous parameters and complex hydraulic motion at the vicinity of the structure, De Waal et al. (1996) mentions that a numerical approach to wave overtopping is not feasible and thus physical modelling is essential.

Physical models are classified as miniature reproductions of a physical system (Hughes, 1993) and are used as a tool to provide optimal solutions both economically and technically. With a defence structure that induces highly turbulent, reflective and chaotic processes like HPC, a physical model portrays an accurate representation of the scenario, by which numerical models cannot. Physical modelling provides tangible representations of the analysis of structures providing a better understanding in the physical process being tested, rather than just relying on mathematical analysis. With the complexity of the breaking process at the toe of the structure, wave impacts are still not properly understood and Bullock et al. (2001) mentions that laboratory experiments help gain a wider understanding on this process especially when testing in a wave flume with transparent sides.

Physical models provide the opportunity to examine coastal phenomena that are beyond analytical skills (Hughes,1993). Furthermore, constructing a physical model provides instantaneous visual feedback and Kamphuis (1991) noted that observing a physical model in action often gives the experimenter an insight into the natural processes which in turn focuses the study and reduces testing periods.

Most numerical models involve a simplified representation of the physics of processes presented in the equations. Mathematical models highlight the important problems but physical models offer the chance to monitor, measure and alter them in a controlled environment (Hughes, 1993). With guidance provided by EurOtop (2016) it is noted that empirical methods can lead to discrepancies in overtopping discharge due to the inability to include all parameters and therefore will not be predicted with the same accuracy as model tests that are structure-specific. A study by Douglass (1984), concluded that overtopping rates that have been empirically derived, are only taken as being within a factor of 1-3 of the actual overtopping rate.

In most hydraulic models, Gōda (2010) mentions that tests concerning surface waves, viscosity and surface tension of water usually do not play significant roles as they are so small and thus can be neglected, leaving inertia and gravitational forces as the governing forces. Thus both the Froude and Reynolds scale are very important when scaling a model, however both cannot be used simultaneously according to Hughes (1993) so it must be determined which force between gravity and viscosity is dominating in the system. In most situations, the Froude law is implemented as gravity plays the most dominant role and the Reynolds law is used to validate the physical model.

When carrying out physical modelling, there are 2 main limiting effects that can affect the outcome of the experiment.

Scale Effects

Burcharth and Andersen (2009) state that scale effects occur *due to incorrect reproduction in the model of the prototype ratios between relevant forces.* In models that are smaller than the prototype, it is never possible to simulate all relevant variables with an accurate affiliation to one another and thus the model is not a perfect replica which induces scale effects (Miles, 2017).

Gōda (2010) mentions the main scale effect that overtopping model tests seem to underestimate is the rate of overtopping when the volume is small. Two experiments carried out by Sakakiyama and Kajima (1997) and Kortenhaus et al. (2005) conclude that the overtopping rate is generally less in the model than prototype. Gōda (2010) further mentions that this scale effect has originated from the roughness resistance due to viscosity and the surface tension of water. However, Hamill (2014) and Heller (2011) mention that surface tension is not normally significant, provided water depths > 20mm and wave periods > 0.35s. Scale effects create a damping effect and parameters including relative wave height and discharge are normally smaller in the model than in the prototype as the fluid forces are more dominant.

A common scale effect during physical testing occurs when water drops in the air are not to scale and too big in the model and therefore does not provide an accurate representation. Bubbles formed in freshwater as oppose to seawater, tend to be larger causing them to coalesce more easily. With large bubbles more buoyant than small bubbles, they rise through the water more rapidly leading to air escaping quicker from freshwater than from seawater. The use of freshwater as oppose to seawater alters the percentage and persistence of air bubbles in the water thus changing compressibility during impacts however Bruce et al. (2002) importantly mentions that there is no evidence for this effect to alter overtopping processes. Bullock et al. (2001) indicates that physical testing of hydraulic models is invariably conducted using freshwater and this introduces a ‘scale’ effect as air behaves differently in freshwater than in seawater however Hughes (1993) mentions that this effect is small.

Following on, the influence of wind depends on the shear stress on the water surface and therefore the shear velocity of the wind should be to scale. A common scale effect in replicated models is that turbulent forces are larger in the scale model than in the prototype not providing an accurate representation (Hughes, 1993).

Most hydraulic models are scaled accordingly to Froude’s law and consequently, friction forces, elasticity effects and surface tension forces are neglected for most models (Van de Meer et al., 2009). To reduce the likelihood of scale effects, the laws of similitude should be applied which governs the model to mimic the prototype performance as realistically as possible. These include geometric similarity (model lengths are in the same ratio to those in the prototype), kinematic similarity (similarity of motions) and dynamic similarity (similarity of forces). A large scale ratio creates a larger deviation in forces but Heller (2011) goes on to mention that even though scale effects increase with a larger scale, there is no given scale that dictates whether or not scale effects can or cannot be neglected. Hughes (1993) concludes that the best method against scale effects is to build the model as large as possible.

Model Effects

EurOtop (2016) and Burcharth and Andersen (2009) state that model effects originate from the incorrect reproduction of the prototypes geometry and waves or the boundary conditions of the wave flume (side walls, wave paddle). The principal

source of these model effects is due to wave generation and wave absorption. These boundaries constrain the hydrodynamics, invalidate measurements and create a finite width of flow. As waves are generated and propagate down the flume, some of this energy is reflected seaward and then combines with the incoming waves and reflected back to the structure forming cross waves and in turn, over-estimating the effects of overtopping. In nature, these reflected waves would continue out to the ocean. This mechanical wave generation creates unwanted nonlinear effects in the form of higher harmonics or longer waves. However this effect was mitigated against by the wave paddle having an active wave absorption system to absorb the unwanted reflected wave energy.

A common model effect arises from the inability to create realistic surrounding conditions e.g. when unidirectional waves are generated in the model to mimic oblique waves that occur in reality (Hughes, 1993). These forcing functions and boundary conditions that occur in nature are not included in the physical model. For example, wind may generate significant nearshore circulation currents whereas during physical modelling, this ability is absent. Furthermore, the inability to reproduce the bathymetry in terms of roughness and geometry induces another model effect that reduces the accuracy of the experiment.

Kortenhaus et al. (2005) mentions that physical modelling methods have advanced but influences of model effects are still present. Oumeraci (1999) pointed out that considerable research is needed to minimise model effects. De Rouck et al. (2005) concludes that one of the main objectives of the research project CLASH (Crest Level Assessment of Coastal Structures), is to resolve the issue of scale and model effects for wave overtopping and improve the reliability of physical modelling.

Hinkley Point C

Hinkley Point C nuclear power station is an on-going project to construct a 3,200 MWe nuclear power station (Revolvy, 2017). The plant has an estimated construction cost of £18 billion with the seawall contributing roughly £52 million.

The seawall is a vertical, gravity mass concrete structure 770 metres long and spans the foreshore of the HPC site from east to west - it will approximately be aligned with the existing cliff that is retreating at an assumed rate of 0.5 m/year. A precast concrete wave return sits on the crest of the wall to a level of 13.50m AOD. Rock armour will be provided to protect the toe of the wall from scour and beach lowering. The design life for the proposed coastal defence structure is 100 years which includes 60 years for the operational plus 40 years of decommissioning.

Previous Wind Related Literature

Extensive research has been conducted on the mean overtopping discharge over various designed seawalls however there is very sparse literature available when assessing the combined effect wind has on overtopping and the distance travelled of this discharge (Allsop et al., 2005).

Physical models have been conducted by Pullen et al. (2009) and de Waal et al. (1996) who experienced similar challenges with regards to scaling wind as the surface tension, viscosity and droplet sizes are the same for both the prototype and model. These spray trajectories should have been modelled using Reynolds scaling, however this is incompatible when using Froude scaling. Similar testing carried out by Ward (1998) concluded that the use of wind in physical models produces higher overtopping rates due to scaling effects and should not be included as wind cannot accurately reproduce the prototype parameters. Kortenhaus et al. (2005) and De Rouck et al. (2005) agree and further add that previously conducted laboratory studies have taken place without the effect of wind predominantly due to considerable scaling difficulties or pre-misconceptions and conclude that wind will not increase wave overtopping discharges. However, Allsop et al. (2005) mentions that the effects of wind can increase discharge by up to 3 times so the incorporation of wind is a necessity when assessing overtopping discharge. With previous literature conducted by De Rouck et al. (2005) and Allsop et al. (2005), the consensus suggests that wind affects lower overtopping volumes. An experiment conducted by De Waal et al. (1996) used a physical model set up with a paddle wheel to generate wind. It was concluded that the paddle wheel was 90% effective at “pushing” the overtopping over the crest of the seawall proving the impact wind has on overtopping especially in flume based experiments.

Further research is still warranted on discharge distances to ameliorate safety behind seawalls. Ward, Wibner and Zhang (1997) did carry out an experiment that focused on the link between generated winds and spatial distribution and reiterated that small overtopping discharges are affected more than large discharges. The droplets generated by splash and spray in this experiment flattened causing higher drag coefficients, increasing the distance the droplets were carried by wind over the crest. These droplets, although small, are still potential hazards to the public and vehicles. Holistically, there have been very little regards to the influence and quantification of wind effects on a scaled coastal structure and Allsop et al. (2005) mentions that more data is required to quantify spatial effects on overtopping hence this experiment.

With HPC aiming to become one of the UK’s leading producers of electricity, the need to protect, preserve and maintain the area is of high importance and hence the requirement of this study. The location of the wall is amongst one of the highest tidal ranges in the world and this coupled with the effects of climate change and sporadic winds, warrant the need for an accurate and systematic approach in the form of physical modelling.

Physical Model Methodology

This section outlines the methods utilised and adapted to carry out the physical experiment using knowledge gained in Section 2 and transforming it into the practicalities of conducting a physical model test.

Overview
Overtopping at structures is a highly complex process – one where analytical methods in the form of numerical and physical modelling are still being developed.

With the experiment aiming to identify how the rate of overtopping and spatial distribution of the overtopped water is influenced by onshore wind speeds, 4 catchment buckets were fitted landward side of the seawall. These were equally spaced and scaled appropriately to provide an accurate and realistic representation of the hazards behind the wall. This experiment was carried out at the COAST laboratory where a model was designed, constructed and operated in a 35m wave flume. A 1:25 scale was applied to the wall and rock armour at the toe taking into account boundary conditions posed by the prototype dimensions, laboratory space and practical considerations such as water depth.

Irregular waves are more representative of actual sea states than regular, however the latter are easier to replicate in a small-scale wave flume (Weller, Stallard and Stansby, 2010). Furthermore, Hunt (2003) adds that regular waves do not provide a realistic scenario in terms of shape or regularity but in comparison, irregular testing requires more time and may not always be feasible. With these drawbacks, as evidenced by Pearson et al. (2005), coastal engineers use a combination of regular and irregular waves during physical modelling to investigate overtopping of coastal structures hence the decision in this experiment.

Physical Model Construction
A seawall of dimensions 0.38m high and 0.59m wide was built using 12mm thick marine plywood. The model structure was designed and constructed to have geometries and wave reflectance properties similar to the prototype. To reduce the effect of wave transmission around the structure and prevent movement under wave loading as mentioned by Hughes (1993), the model was specifically designed to be tight fit. Behind the model, the buckets stretched back 0.6m equating to 15m in the prototype which modelled hazards in the form of a footpath (Bucket 1), fence line (Bucket 2) and retaining structure (Buckets 3 and 4). The fronting foreshore slope used a previously constructed wooden ramp of 2.8m long with an angle of 8˚ to mimic the prototypes bathymetry. CIRIA (2007) mentions that it is essential to not only provide accurate waves at the toe of structures but also necessary to model a part of the foreshore bathymetry and this is done with a fixed bed model used in this case.

With previous flume based models, there had been issues with buoyancy once the water had been introduced so a total of 120kg was placed beneath the model and at the toe of the ramp, a weight was placed to prevent lifting. The structure itself was further fixed and clamped to a previously constructed template to ensure no sliding motion occurred on the smoothed surfaced flume.

Construction methods
As oppose to past projects, new construction methods were proposed to build the seawall model whilst taking into account buildability, cost and availability of materials

within the University. Below outlines the methods used to construct the seawall, collection buckets and in-situ wave gauges:

Sea wall

With a DXF file provided of the cross section of the wall, through the means of water jet, seawall offcuts were produced, aligned with the use of dowels and glued. Several coats of varnish were applied and gaps were filled using filler. This method was adopted to obtain an accurate representation for the geometry of the bullnose whilst maintaining the structural strength. These can be seen in figures 3, 4, 5 and Appendix C.

Figure 3: Seawall offcuts produced from an 8m x 4m sheet of 12mm plywood

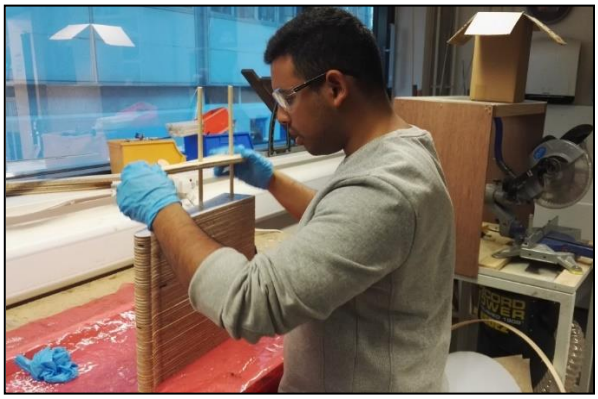

Figure 4: Gluing the offcuts and aligning them with the use of dowels

Figure 5: Fully varnished and completed seawall model

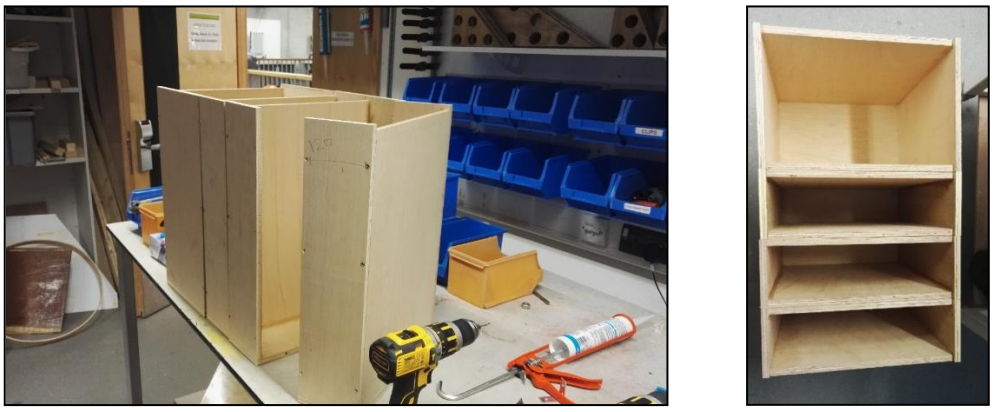

Figure 6: Plan view of collection buckets

Collection buckets

In previous years, plastic collection buckets were used and weighed after each run to obtain an overtopping discharge however this method was deemed time-consuming and inaccurate. This method was adapted and wooden collection buckets were used and scaled to mimic potential hazards in reality. The boxes spanned 60% of the full width of the flume to reduce the effect of reflection and friction from the side walls thus reducing the model effects as mentioned in Section 2.7.2. They had a full width of 0.36m with a depth of 0.5m. Each box therefore provided a full potential volume of $0.022m^3$ for the first 3 buckets and $0.043m^3$ for the last which equated to 22L and 43L respectively.

Wave gauges

In-situ wave gauges were used to provide an instantaneous and in-situ reading rather than weighing the boxes individually, a technique successfully utilised by Pearson et al. (2005). The gauge operates by measuring the resistance of the water between a pair of parallel conducting rods (www4.edesign.co.uk, 2018). The gauge itself was laser cut and copper strips were attached but unfortunately were ineffective despite prior testing (Figure 8) and wave probes were used. The wave probes were a simple, robust and low cost alternative that provided a set of reliable results.

In the flume, 4 wave probes were deployed seaward of the wall and 4 leeward of the wall in each collection bucket. The placement of each wave probe is shown in figure 9. The positioning of the wave probes were chosen for reflection analysis.

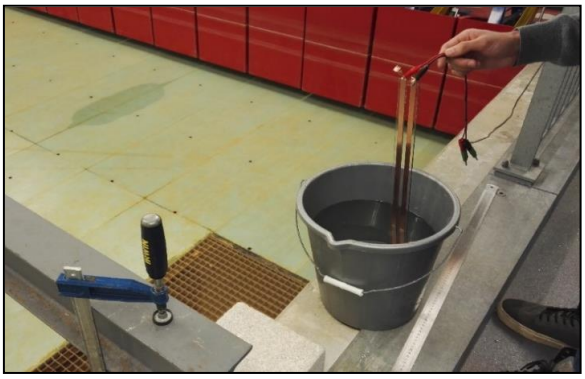

Figure 7: Testing the wave gauges prior to experiment

Figure 8: Wave gauges with copper tape attached

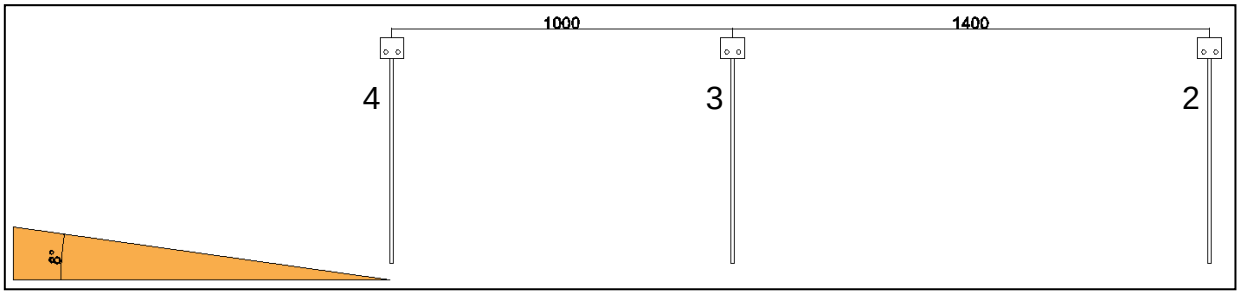

Figure 9: Positioning of wave gauges

Resistance between the rods is proportional to the immersion depth and computer software was used to confirm the water level from measured voltage. The wave probes were connected to a controller that had a measurement rate of 128Hz and were calibrated everyday due to changes in resistance in the water caused by temperature.

Design Conditions

Water Levels

With a lack of published data on HPC, extreme water levels were obtained from an amended tidal curve process using guidance provided by the Environmental Agency and tide times using the Admiral Tide Tables. Three components were required to generate a design tide curve – an extreme sea level, a base astronomical tide and a surge component. This process is fully outlined in Appendix D.

Three water levels were tested based upon a 1 in 1, 1 in 100 and 1 in 1000 storm surge and when scaled were 0.534m and 0.56m and 0.574m from the base of the flume (Figure 10) with a respective crest freeboard of 0.226m, 0.256m and 0.3m.

The original plan was to test Mean High Water Springs however it was observed from test waves that shoaling occurred further down the beach and in turn the waves broke. This meant a lot of the wave's energy had dissipated before reaching the seawall and little, if any, overtopping occurred at all. From this observation, it was

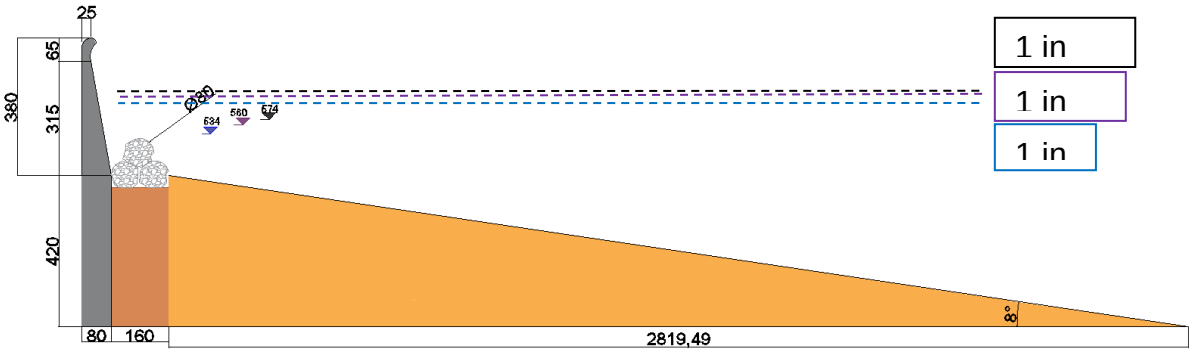

Figure 10: Cross section of the model setup with scaled water levels

decided to increase the water levels as the main phenomenon being measured was not observed.

Wave Conditions

The wave spectra that ran in the flume was a combination of 7 frequencies assisted with 7 wind conditions (including no wind) creating a matrix of 49 combinations that ran at 3 different water levels. The waves generated by the paddle were of the JONSWAP wave spectrum meaning the spectrum was fetch limited. The paddle used is known as a Piston wavemaker and was effective as it was able to generate waves without generating any back waves and therefore capable of measuring incoming waves and correcting paddle motion to absorb them. The computer programme used to control the paddle was "Njord Wave Synthesis" using the following inputs: type of spectrum, peak frequency, water level, significant wave height and duration.

Table 1 outlines the prototype and model wave heights and wave frequency for the regular and irregular waves used based on the following methods and Froude scaling:

Table 1: Prototype and model wave conditions

Wave Condition (WC)					
WC	Irregular/Regular	Wave Height (m)		Wave Frequency (Hz)	
		Prototype	Model	Prototype	Model
1	R	2.26	0.09	0.10	0.50
2	R	2.26	0.09	0.12	0.60
3	R	2.26	0.09	0.14	0.70
4	R	2.26	0.09	0.16	0.80
5	R	2.26	0.09	0.18	0.90
6	I	3.2	0.128	0.15	0.75
7	I	5	0.2	0.12	0.59

Using prior extreme wave analysis conducted by HR Wallingford, the wave heights and wave periods were obtained for the irregular waves and scaled down. Using the energy equivalence equation, the equivalence between regular waves and irregular waves were calculated whilst keeping the sea state wave energy (E) and wave power (J) constant (Blanco et al., 2015):

$$E = \rho g \int_0^\infty S(f)df \Rightarrow \left\{ \begin{matrix} \text{irregular} \\ \text{wave} \end{matrix} \rightarrow E = \rho g \frac{H_s^{\,2}}{16} \right\} \Rightarrow \sqrt{2} \cdot H_{reg} = H_s \qquad (5)$$

$$J = \rho g \int_0^\infty c_g(f) \cdot S(f)df \Rightarrow \left\{ \begin{matrix} \text{irregular} \\ \text{wave} \end{matrix} \rightarrow J = \rho g^2 \frac{T_{-1,0} \cdot H_s^{\,2}}{64\pi} \right\} \Rightarrow T_{reg} = T_{-1,0} \qquad (6)$$

Where: **ρ** is the ocean water density (kg/m^3); **S(f)** is the energy wave spectrum (m^2/Hz)

g is the gravity constant (m/s^2); $\mathbf{c_g}$ is the group velocity (m/s); $\mathbf{T_{-1,0}}$ is the energy period (s);

The regular wave conditions were based of the 1 in 1 irregular wave condition and the energy equivalence equation was applied to the wave height to produce a regular wave height that under the same frequency had the same energy. The regular waves had the same wave height for comparability. An example calculation is shown in table 2:

Table 2: Energy equivalent example calculation for 0.5Hz

Energy equivalent equation	1 in 1 irregular wave height (Prototype)	Regular wave height (Prototype)	Regular wave height (Model)	Model wave frequency
$H_{reg} = Hs/2^{0.5}$	3.2m	2.26m	0.09m	0.5Hz

The decision to conduct several small tests was based following research conducted by Reis, Neves and Hedges (2008) who recommend that several tests of the same short duration should be undertaken rather than one test with a very long duration and this benefited the time constraints involved. This is seen in Table 3.

Table 3: Regular wave run durations

Model Frequency (Hz)	Time per wave (s)	Number of waves	Time per run (s)	Total time per run (mins)
0.50	2	75	150.0	2.5
0.60	1.7	75	125.0	2.1
0.70	1.4	75	107.1	1.8
0.80	1.3	75	93.8	1.6
0.90	1.1	75	83.3	1.4

Wind Conditions

A large turbo fan was used to replicate the wind created during regular or stormy conditions along the coast. With the fan producing a percentage in terms of blower output, an anemometer was used to measure wind speeds in miles per hour which was then converted into metres per second (m/s). Figure 11 shows the setup of the fan, located 2.3m in front of the wall, at 90° to ensure the wind had minimal impact on the waves and optimal effect on overtopping. Following guidance from Pullen et al. (2009), this placement ensured that the wind did not affect the incident waves, but assisted in 'pushing' the overtopping discharge over the wall.

Figure 11: Wind generator set up

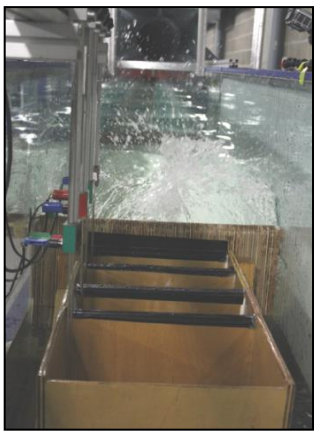

Figure 12: Wind causing splash overtopping into the first collection bucket

To obtain a range of wind speeds, 3 year's worth of wind data at HPC was accumulated, plotted and scaled to identify trends and extreme values which provided a range of values to test between. Prototype wind speeds ranged between 3m/s to 19m/s in roughly 3m/s intervals as seen in Table 4. For the wind speed to be accurately modelled for each run, the fan was calibrated through determining a relationship between the blower and resulting wind.

By incrementally increasing the output of the blower and measuring the output, a graph, figure 14, was drawn from which any chosen wind speed could be produced for a given value. The wind cups were placed at two different positions as seen in figure 13 – one above the crest and one above the rock armour. Position B was used

as it was deemed the optimum position at which most affected the overtopping discharge – the variable being tested.

Table 4: Model and prototype wind speeds

Wind Speed (WS)			
WS	***Fan speed (%)***	***Prototype (m/s)***	***Model (m/s)***
1	0	0	0
2	5	2.5	0.5
3	12	6.65	1.33
4	17	10.95	2.19
5	23	14.45	2.89
6	26	16.1	3.22
7	31	19.85	3.97

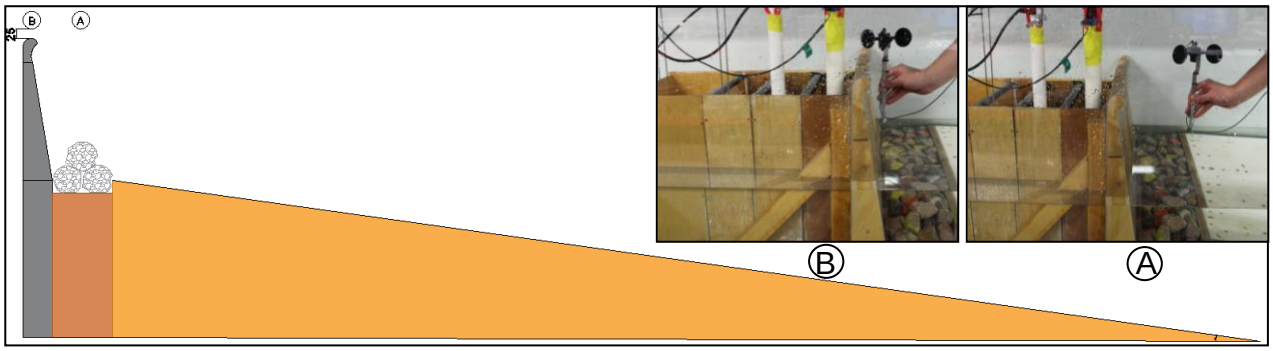

Figure 13: Cross section of model with anemometer positions and experiment snapshots (Measurement took place in the centre of the duct to ensure the flow was consistent enough for the cups to independently turn).

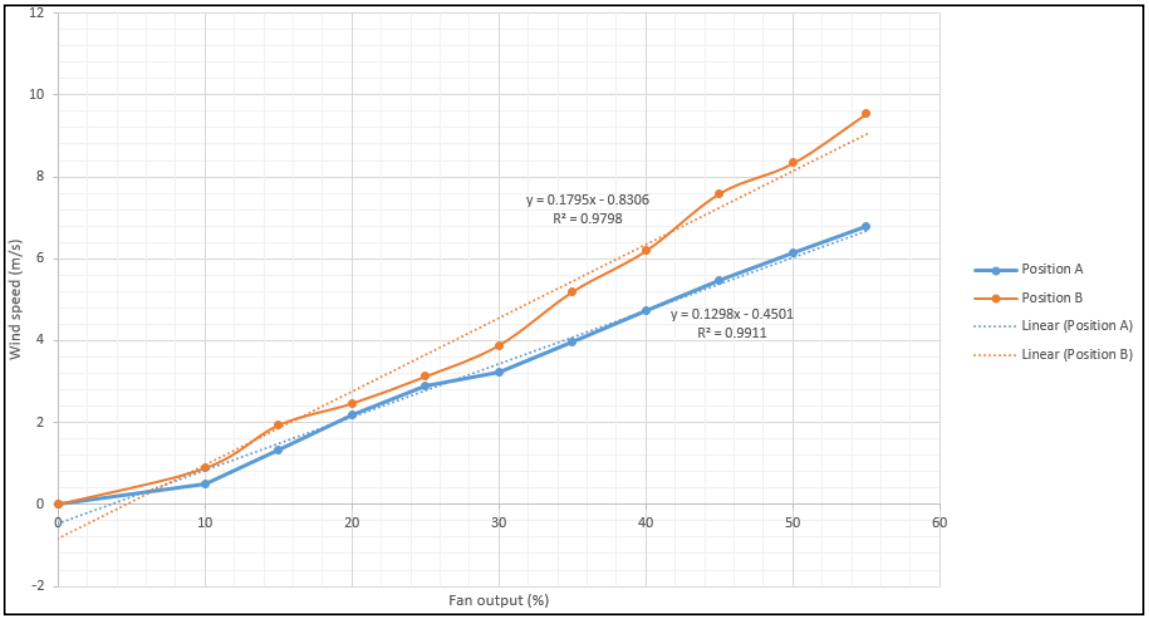

Figure 14: Relationship between fan output and model wind speed

Wind scaling in terms of flow is dominated by Reynolds laws due to the effects of viscosity however due to limited existing information on successfully scaling wind speeds with regards to coastal defence, the field of wind turbine testing and aeronautical experiments was consulted. With guidance provided by Hansen et al. (2014) who used Froude scaling when investigating the effects of wind turbines, it was found that Froude scaling can be used to provide an effective representation of wind forces when scaled, with Reynolds used to validate.

Table 5: Reynolds scaling of wind speeds for model and prototype

	Prototype			Model		
Fan speed (%)	Wind speed (m/s)	Reynolds number	Turbulent/Laminar	Wind speed (m/s)	Reynolds number	Turbulent/Laminar
0	0	0		0	0	
5	2.5	1720287	T	0.5	13762	T
12	6.65	4575963	T	1.33	36608	T
17	10.95	7534857	T	2.19	60279	T
23	14.45	9943258	T	2.89	79546	T
26	16.1	11078648	T	3.22	88629	T
31	19.85	13659078	T	3.97	109273	T

The Froude scaling relationship is valid providing both the Reynolds number remains in the turbulent flow region for both the model and prototype, defined as Re > 4000. It can be seen from Table 6, the Reynolds numbers are greatly within the turbulent flow region. Constructing models at a large scale, ensures that the Reynolds numbers are within a large enough to maintain turbulent flow removing the significance of viscous effects. Once a flow becomes highly turbulent, the viscous forces become less important and gravity becomes the restoring and dominant force, justifying the choice of Froude scaling for wind.

Model setup

The layout of the physical model and the model bathymetry was based on existing seabed surveys and initial CAD drawings. Froude scaling laws were applied to estimate prototype behaviour from observations and measurements in the model. A visual representation of the model setup is provided in Appendix A.

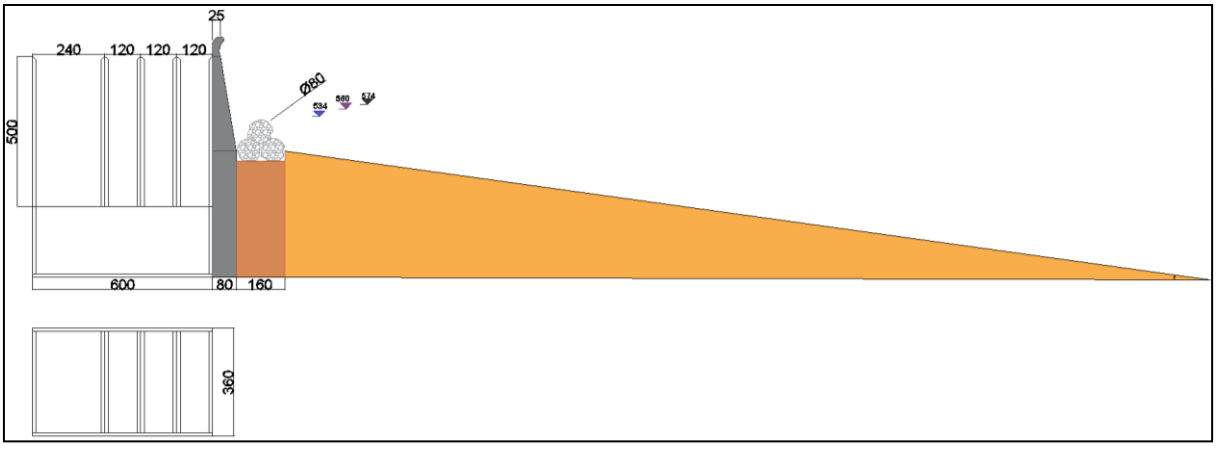

Figure 15: AutoCAD model setup

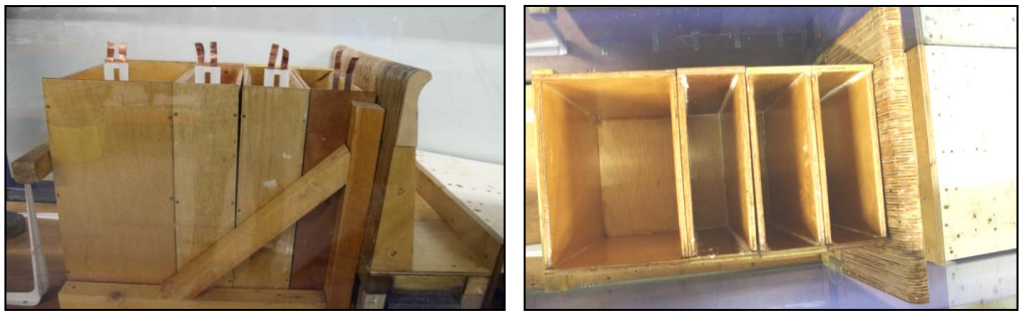

Figure 16: Plan and cross sectional view of experimental setup

Accuracy and Reliability

When conducting physical experiments, there is always an uncertainty with measuring quantities. The reliability of these measurements depends on the accuracy and precision provided by the instrument, coupled with the operators dependability and skill (Hudson et al., 1979). Water depth was measured to the nearest mm whilst overtopping was measured with wave probes. In past experiments, these wave probes exhibited a good linear response and achieved a resolution within 0.1mm (www4.edesign.co.uk, 2018). They were calibrated statically where they were vertically raised and lowered, achieving a strong least squares linear regression. These probes were used based on availability along with advice provided by Hudson et al. (1979) who mentioned that these probes have little obstruction to the wave front leading to no distortion of the resulting discharge. Overtopping resulted in some water droplets remaining on sides of the boxes regardless of the slanted edges, the brackets used to secure the wave probes and on the duct tape used to secure the boxes together. Whilst this was unlikely to affect large overtopping results, small discharges will be affected but will have a negligible effect on the overall accuracy.

There is also a possibility that there could have been a difference between the intended generated wave height caused by software controlling the response of the wave paddle or the aforementioned model effects arising from friction from the sidewalls. These however could be checked by comparing the predicted wave heights with recorded wave heights from the wave probes at the toe of the foreshore ramp. Due to time restrictions repeats of the wave runs were not carried out even though repeat tests demonstrate the capability of a model to produce similar results under similar requirements. Ideally, repeat testing should be carried out to optimize design and develop a better understanding of the underlying theory. With the random nature inherent in flow models, repeat readings may not always provide an improvement in terms of accuracy however are necessary to establish statistical certainty. Within physical modelling, the extent to which these measurement errors impact laboratory results depends on the magnitude of the error relative to experimental errors such as model and scale effects. However, Hughes (1993) and Kamphuis (1991) mention that for small scale models of prototype projects, the quality of the instrument output exceeds the capabilities of the model, which is limited by these aforementioned effects hence the need to ensure that the instrumentation

used is calibrated and tested prior to use is critical to guarantee accurate results and eliminate systematic errors.

Presentation and Analysis of results

This section contains an assessment into the observed trends and the validity of the results, highlighting sources of error and improvements for future testing should a similar experiment be conducted.

Observed Trends

Effect of wind

Seven prototype wind speeds were tested that varied between 0m/s and 20m/s and applied to different wave frequencies and the distances that the overtopped water travelled were recorded, measured and analysed. In general, there was a positive relationship between wind speed and overtopping rate. Figures 17 and 18 demonstrate the relationship between overtopping rate and onshore wind speed at two different water levels – a 1 in 100 and 1 in 1 storm surge. The overtopping rate on the y-axis was used as a means to normalise all the data, apply consistency and comparability between each run. In both cases, the overtopping rate was found to be increasing under the influence of onshore winds. Pre-dominantly for the 1 in 100 water level, it was noticeable that the lower frequency waves produced higher volumes of overtopping due to the location at which the waves were breaking in relation to the seawall toe. These waves broke closer to the seaward toe of the structure which caused an uprush of water in the form of splash or spray as seen in figures 19 and 20. This overtopping discharge was either carried over the wall under its own momentum or driven by onshore wind.

Overtopping rate

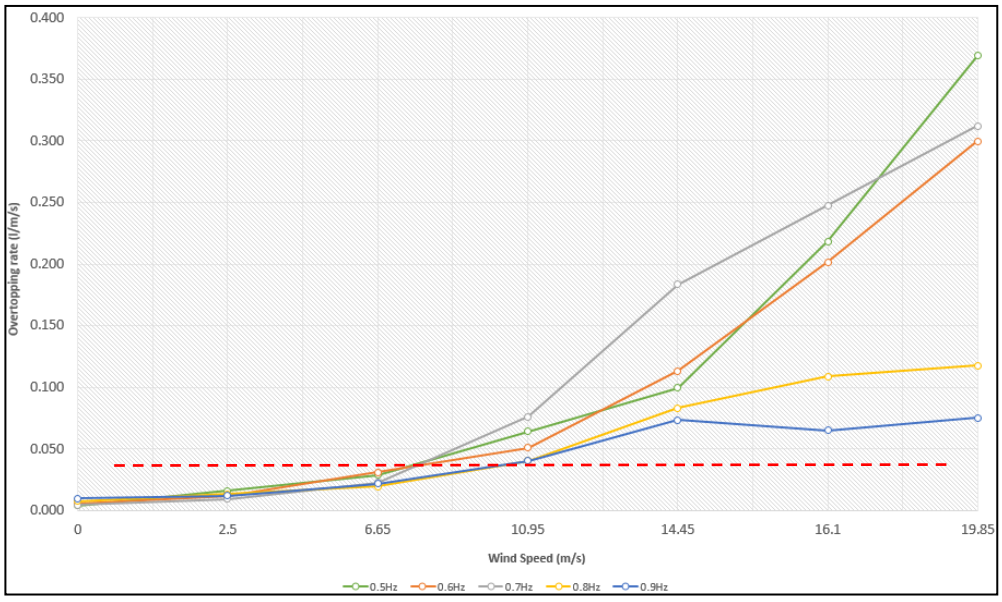

Figure 17: Comparison between overtopping rate against prototype wind speed at 1 In 100 water level for each wave frequency (dotted red line depicts HPC **overtopping rate)**

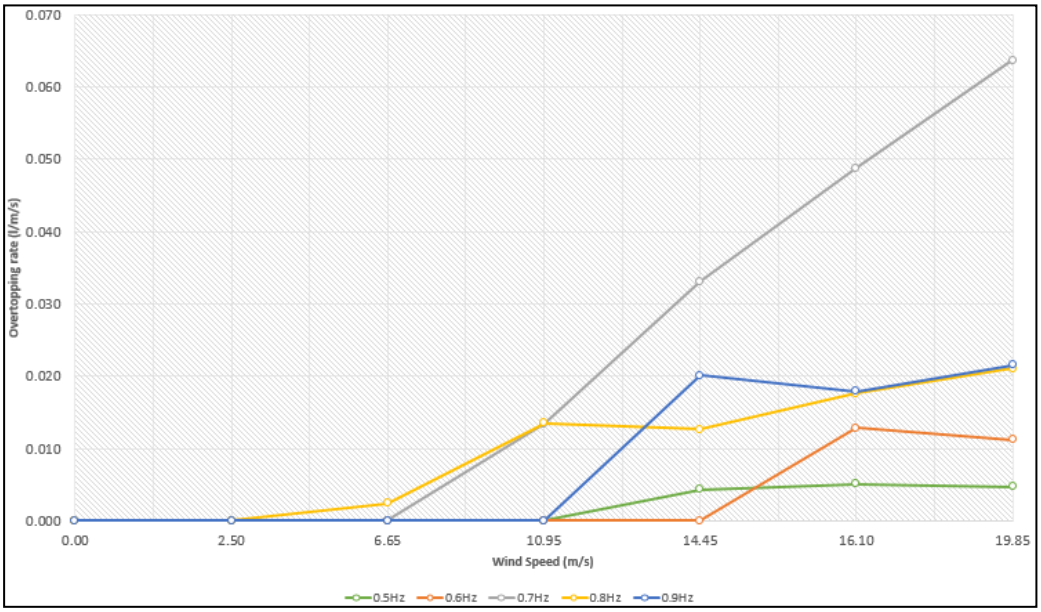

Figure 18: Comparison between overtopping rate against prototype wind speed at 1 In 1 water level for each wave frequency

Figure 19: 0.7Hz at 0m/s wind showing an uprush of aerated water with added time stamp

Figure 20: 0.9Hz at 0m/s wind showing the full effect of the bullnose with added time stamp

Table 6 shows the difference in overtopping rate for all wave frequencies at 3 wind speed categories – Low, Medium and High (based on the Beaufort scale). The highlighted values show the greatest difference in overtopping rate between the two given wind speed values for a specific wave frequency. The lower frequencies, which produced a significant volume of splash, showed greatest change when the higher wind speeds were introduced which is expected as these waves broke closer to the structure causing the generated splash to be pushed over by the higher winds.

Table 6: Difference in overtopping rate for each wave frequency at 3 wind intervals at a 1 in 100 water level

	0.5Hz	0.6Hz	0.7Hz	0.8Hz	0.9Hz
	Difference in overtopping rate (l/m/s)				
0 to 6.65m/s	0.0246	0.0256	0.0184	0.0121	0.0123
6.65 to 14.45m/s	0.0708	0.0826	0.1607	0.0636	0.0517
14.45 to 19.85m/s	0.2699	0.1864	0.1289	0.0346	0.0015

However, the higher frequency waves, which produced a substantial amount of green overtopping with a larger volume, generated the greatest overtopping rate difference at lower wind. From previous literature conducted by De Rouck et al. (2005) and Allsop et al. (2005), as mentioned in the literature review, this effect is expected demonstrating that wind has a greater effect on lower overtopping volumes as oppose to the larger discharges at higher frequency waves however De Waal et al. (1996) goes on to mention that the influence of wind is predominantly affected by the position at which the waves break. This supports the variation in overtopping rate between the varying frequencies and provides an insight as to how the 0.7Hz waves produced the greatest response to wind as seen in Figures 19 and 20.

For the higher frequency waves (0.8Hz-0.9Hz), the waves were predominantly surging, which reflected of the wall, interacting with the incoming waves causing the amplitude to roughly double, giving rise to partial “clapotis” promoting erosion at the toe. This effect is observed in Appendix F. This wave reflection from smooth prototype walls tends to be smaller in the model due to the increased friction thus reducing the magnitude of overtopping that occurs. When comparing the two water levels, the lower water level has a significantly lower overtopping rate purely based of the fact that the wall was sufficiently high, purposely built and well-constructed. The 0.7Hz regular wave produced the highest overtopping rate and at the higher water level, on average, produced an overtopping rate that was 5 times greater than the lower water level, exceeding the tolerable level at HPC.

Both tests displayed the effect of wind, following the steady increase especially up to the speed of 6.65m/s, after which, the overtopping rate increased sharply and rapidly. Especially at the lower frequencies, the overtopping rate then began to slow at the higher wind, demonstrating the numerous effects wind has on frequency. It has been previously detailed by Van de Meer et al. (2016) that wind speed can have a dramatic effect on the increase of splash overtopping – a point well observed.

For pedestrian safety, designers have recommended an overtopping rate limited to 0.1l/s/m to avoid excessive erosion behind the seawall. This overtopping rate was exceeded for the lower frequency waves when the wind speed reached roughly 12.5m/s. In reality if this did occur, the effectiveness of raising the seawall crest level as part of a managed adaptability strategy would have to be evaluated.

Figures 21, 22 and 23 demonstrate the effect of spatial distribution. It is evident that the proportion of wave overtopping passing the crest decreases with landward distance when no wind is present however increases with the generation of wind. With this increase, generally so does the quantity and distance travelled of the overtopped volume. When analysing Figure 21, specifically buckets 3 and 4 for 0.5Hz and 0.6Hz, it is evident that a greater percentage of water reached bucket 4 and this is based on the fact that it was twice the volume and thus able to collect water over a greater distance. Figure 23 shows similar trends but is more exaggerated as a result of the increased wind. From the literature review, with guidance from Ward, Wibner and Zhang, (1997) it is mentioned that when wind is introduced, the overtopped water flattens, causing a higher drag coefficient which increases the distance the discharge travels as evident in this experiment.

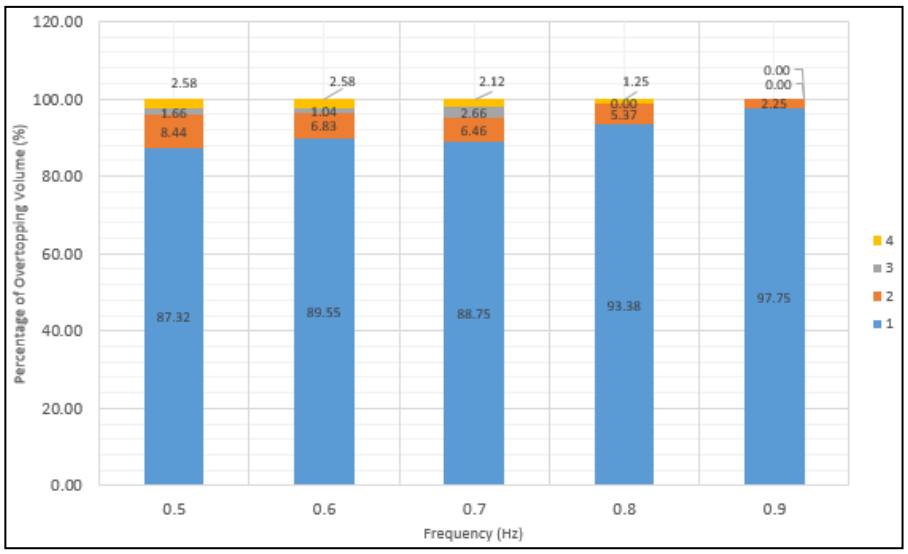

Figure 21: Comparison between percentage of overtopping volume against frequency of waves at 1 in 100 water level with 0m/s wind for the four collection buckets

Spatial Distribution of the overtopped water

When no wind was present, 97.1% of the total collected volume entered into the first 2 collection buckets and interestingly the 0.8Hz and 0.9Hz waves produced the greatest volume of water in these buckets, attributed to the phenomenon of green overtopping as a result of surging waves. These waves did not break at the toe and thus splash overtopping was not generated. This phenomenon is an effect not wanted, as a reflective seawall with primary function of protecting a power station and footpath, aims to eliminate green overtopping, minimising the effects of flooding. Disregarding wind, geometrically the slope majorly affected the spatial distribution of overtopping water. With this 1:7 slope classified as mild using guidance from EurOtop (2016), the waves lost more energy to breaking with less energy reflected. This breaking at the toe was pushed over at the higher wind speeds to increase the overtopping rate into buckets 3 and 4 as seen in figure 23. This combination of

breaking and reflection on the seaward slopes affected the horizontal velocity, a key parameter affecting the landward spatial distribution of water (Peng and Zou, 2011).

Figure 23 shows that with increased wind speed, buckets 3 and 4 attained a total of 32.4% as oppose to 2.5% at no wind proving the relationship between wind and distance of discharge. The 0.8Hz and 0.9Hz waves produced the greatest reduction in percentage of volume with increasing wind.

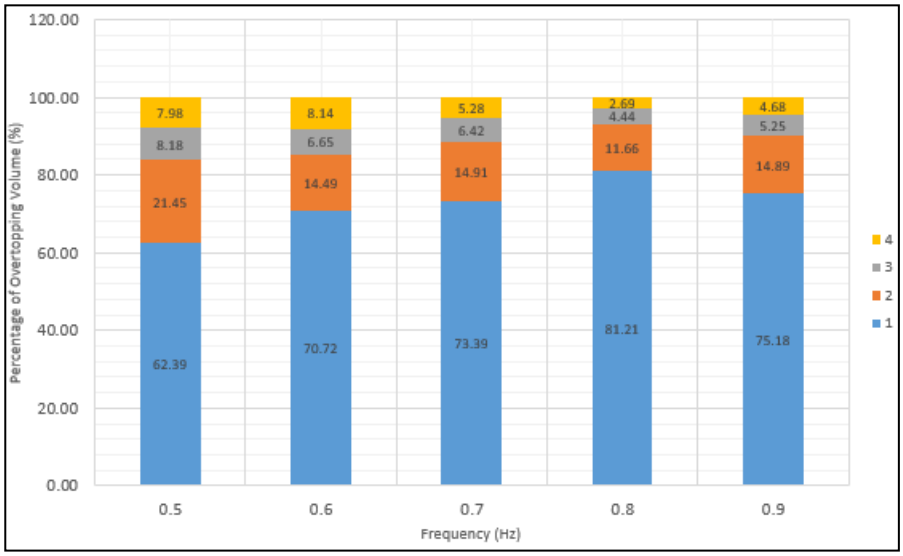

Figure 22: Comparison between percentage of overtopping volume against frequency of waves at 1 in 100 water level with 10m/s wind for the four collection buckets

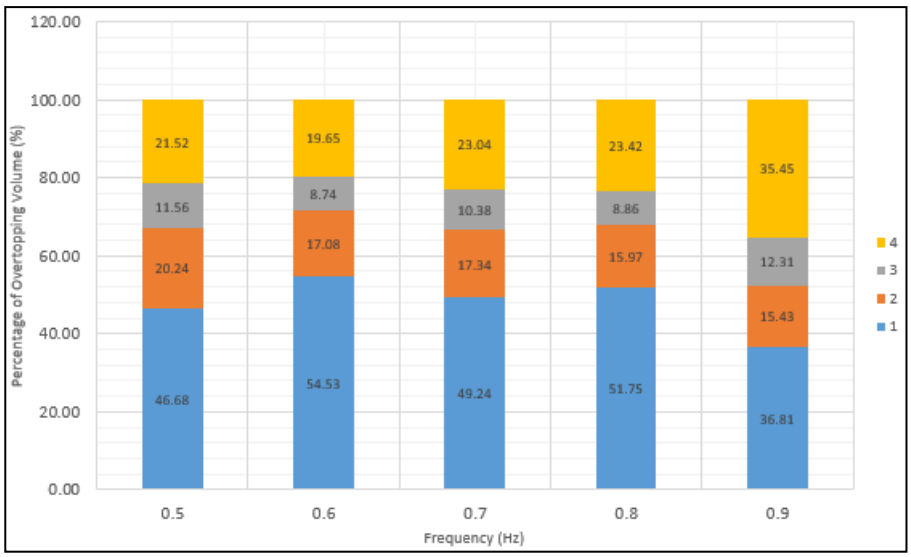

Figure 23: Comparison between percentage of overtopping volume against frequency of waves at 1 in 100 water level with 20m/s wind for the four collection buckets

Respectively, there was a 42% and 61% reduction of volume into bucket 1 but a 22% and 35% increase into bucket 4. This shows that green overtopping occurring initially transformed into splash with an increase in wind thus travelling further. These higher frequency waves showed a greatest response to wind speed.

The sequences in figure 24 and 25 demonstrate the proximity of the scaled footpath, ramps and other retaining structures hence the danger for public and workers. When analysing the 0.7Hz wave, the results showed that wind had the effect of increasing the overtopping volume by 46 times relative to zero wind conditions.

Figure 24: 0.7Hz wave with 0m/s wind showing minimal overtopping with added time stamp

Figure 25: 0.7Hz wave with 4m/s wind showing significant splash overtopping with added time stamp

Regular and Irregular wave trends

Both regular and irregular wave patterns were used to evaluate the design of the Hinkley Point C sea wall based on past literature by Pearson et al. (2005). Regular waves provided an insight into the potential trends such as the effects of frequency with wind whereas irregular waves helped analyse the design state.

Wave Breaking

It is of extreme importance that wave breaking in the prototype, produces the same hydrodynamic response as in the model though small scale experiments like this suffer a scale effect in regards to surface tension (Hughes, 1993), reducing the credibility of the outcome. However, contradictorily, Le Mehaute (1976) argues through systematic experiments that pressures exhibited in the model are in similitude with the prototype.It was apparent that this structure, when modelled, experienced waves breaking directly in the form of short duration, high intensity shock pressures. This extreme breaking, more occurring at the lower frequencies, led to severe overtopping. As evidenced by EurOtop (2016), the results in Table 7 are

expected for a vertical wall, and are likely to experience impulsive breaking where the overtopping is sudden and violent at greater velocities.

Table 7: impulsive wave calculation of the parameter h* at 1 in 100 water level (EurOtop, 2007)

Frequency (Hz)	Tm	Significant wave height (m)	PI()	g	1.35	h*	I/NI
0.5	10.000	2.26	3.142	9.81	1.35	0.047	Impulsive
0.6	8.333	2.26	3.142	9.81	1.35	0.067	Impulsive
0.7	7.140	2.26	3.142	9.81	1.35	0.092	Impulsive
0.8	6.253	2.26	3.142	9.81	1.35	0.120	Impulsive
0.9	5.553	2.26	3.142	9.81	1.35	0.152	Impulsive

To assess the effective design load, a dynamic analysis is required. Overtopping rates are strongly determined by how violent wave breaking at the structure is and this is why determining whether conditions are impulsive or non-impulsive are so important. When h* < 0.2, as in this case, impacting waves predominate. These impulsive conditions are caused when some waves are larger in relation to the local water depths causing the waves to violently break against the structure, with the discharge characterised by an up-rushing jet of highly aerated water as seen in Figure 35.

Lundgren (1969) described three types of breaking waveforms that cause shock pressure intensities greater than pressures induced by similar sized non-breaking waves: compression shock, hammer shock and ventilated shock. These are illustrated in figure 37 and although significant, are not always considered during design leading to substantial damage despite impulsive loading yielding loads 10-50 times greater than non-impulsive loading as mentioned by Bruce et al. (2005):

Figure 26: Impact forces against the face of the vertical seawall

Irregular wave trends

Figure 27 shows a comparison of the irregular waves at various water levels and outlines the aforementioned relationship between wind speed and overtopping rate. It shows a similar trend as before and exaggerates the changes in wave conditions

from a 1 in 1 storm event to a 1 in 100 storm event. This leads to the conclusion that storm events with different intensities and conditions, have a significant influence on the overtopping rate. Furthermore, the results demonstrate the irregular 1 in 100 wave conditions with a larger wave height, at each water level, shows greatest response to wind at 14m/s whereas the 1 in 1 wave conditions beginsto deteriorate. This increase in wave height can be attributed to a greater uprush of water caused by larger wave conditions, hence providing a greater area upon which the wind acts, carrying greater volumes over the crest as evident in Figure 27. These results are more relatable to the outcome of the study.

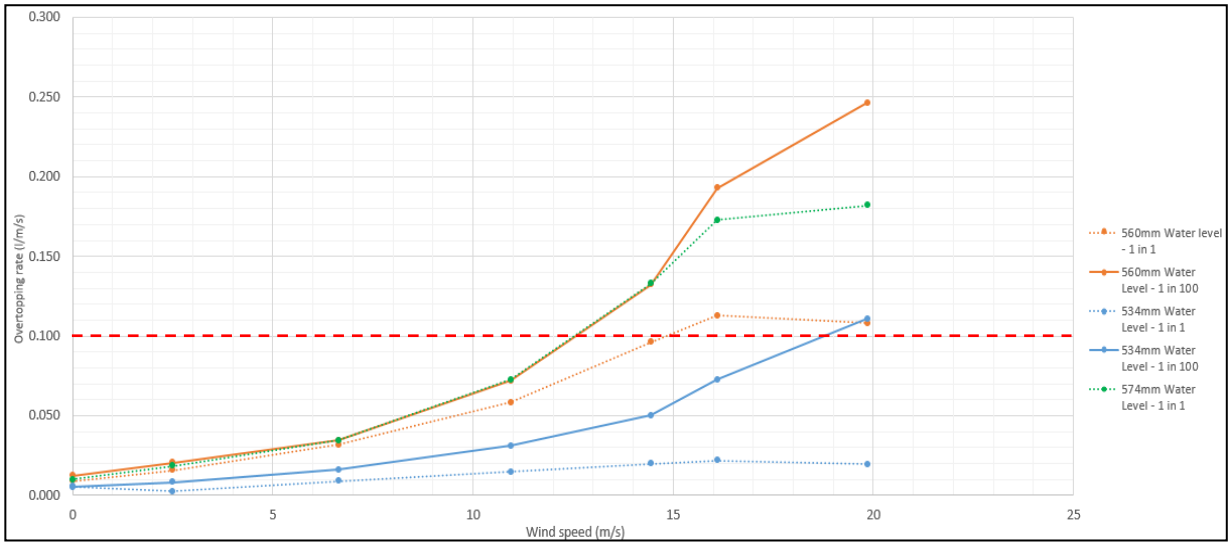

Figure 27: Comparison of wind speed against overtopping rate for irregular waves (dotted red line depicts HPC overtopping rate)

VARYING FREQUENCIES

At the 1 in 100 water level, general trend lines were set to demonstrate the exponential relationship between wind speed and overtopping volume. This exponential relationship can be explained as it is known that the force, wind, exerted over a given area is proportional to the square of its velocity (Xu & Bowen, 1994). Hence, as the wind speed increases, so does the force exerted upon the up-rushing water, carrying greater volumes over the crest. These exponential trend lines help explain the difference between the wave frequencies against increasing wind speed.

The 0.8Hz and 0.9Hz waves shows a trend explained by de Waal et al. (1996) and Pullen et al. (2008) who found that even when the wind enhancement of overtopping is large, the discharge is small. This graph shows that the lower frequency waves are producing a greater volume of overtopping as oppose to the higher frequency waves. It was noticeable that the peak frequency was between the 0.6-0.7Hz region. Waves at these frequencies broke closest to the toe and rock armour thus producing a large volume of water that was pushed up and over with increasing wind.

These results are for regular waves and thus cannot solely be used to analyse the performance of the structure. Hughes (1993) mentions that these regular waves are

linearly superimposed to comprise the given sea state and so regular waves do not provide an accurate representation however have provided an insight into the

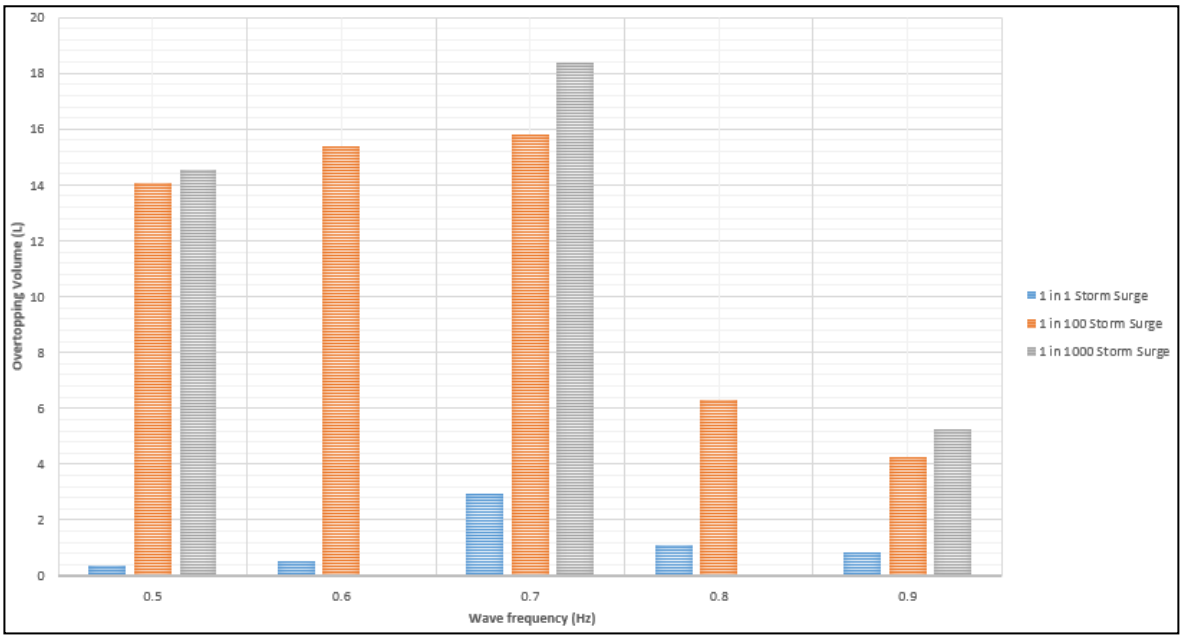

Figure 28: Wind speed against overtopping volume for each varying frequency at 1 in 100 water level

general trends.

Water depth comparison

Figure 29 is a discrete bar chart that has been used to visualise the comparison between all storm surges and it is noticeable that 0.7Hz at each water level produces the greatest overtopping volume. This wave frequency was noticed to break at the toe of the structure and thus had most interaction with the rock armour.

This interaction led to an uprush of aerated water, increasing the overall overtopping volume in all cases.

An increase from the 1 in 1 water level to the 1 in 100, equates to a 0.85m prototype increase in water level which caused an increase up to 38 times for the 0.5Hz wave whereas the water level increase from a 1 in 100 to a 1 in 1000 equates to 0.43m and causes the overtopping volume to increase by only 1.2 times. This relationship is similar than that explained by Iwagaki, Tsuchiya and Inoue (1966) who mention that from their results the effect of wind on wave overtopping varies considerably and is extremely sensitive with the relative water depth at the toe of a seawall. With increased sea level, a threshold will be exceeded when wave overtopping will become a significant hazard due to the increased frequency of extreme storm events. This increase reduces the crest freeboard and increases the phenomenon of green overtopping, a point observed especially at the higher water levels.

This structure has been designed for a 1 in 100 year storm event and raises questions as to whether the wall has been designed appropriately. These water level predictions have been based on the joint probability predictions which may not be as accurate especially with the extensive tidal range present however it does provide statistical evidence that this wall is unlikely to provide substantial protection against extreme storm events.

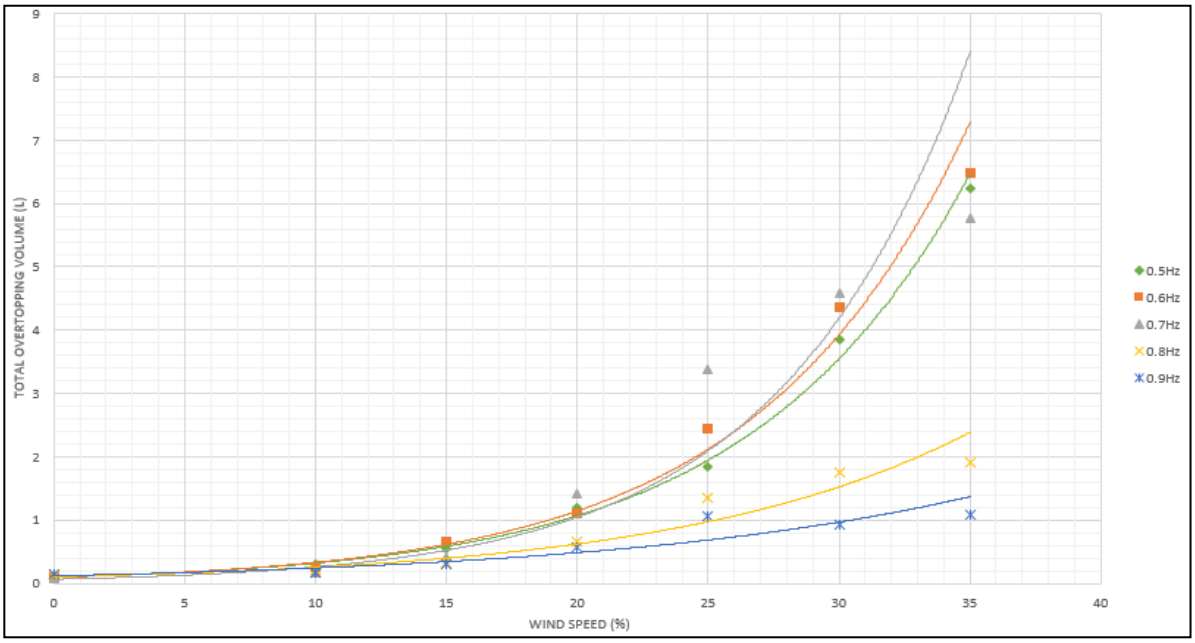

Figure 29: Comparison between wave frequency and overtopping volume at each water depth tested (It should be noted that at the highest water level, 0.6Hz and 0.8Hz waves were not tested due to time restrictions)

Visual Observations

During wave simulations, it was noticeable that waves were breaking at various points around the toe of the foreshore and on the foreshore itself due to depth-induced breaking. However, it became obvious that this was due to the flexibility of the seabed despite reinforcing it with sealant. This flexibility forced the bed to bend under the force of the waves which in turn raised the water level causing waves to break closer to the toe at times. This would have caused inconsistent wave propagation and breaking effects between the spectra. This was noticed towards the end of the testing period and was deemed not to have a major impact on the overall overtopping volumes however in future a more dense material should be used to act as a foreshore but with the availability of materials, this deemed the most effective option. Furthermore, it was extremely noticeable the influence of the sidewalls on the incoming waves as seen in figure 30.

These waves were attenuated by the internal friction from the flume sides and the bottom boundary layer friction arising from water viscosity. This friction causes a reduction in the wave height of the waves reaching the structure which reduces the accuracy of the model when compared to the prototype.

Figure 30: Friction from the side walls affecting incoming waves

Rock Armour Stability

The armour placed along the toe of the structure was through a relatively random process to replicate the prototypes method. Only a few rocks were chosen at a time to suppress the tendency to select best-fit units and thereby artificially increase stability (Hann, 2018). Through an overlay photograph technique before and after each run, images were superimposed and compared to identify rock displacement and rocking. Hughes (1993) mentions that this rocking can cause breakage of the units into smaller pieces making them more easily removed by waves thus exposing the face of the structure. The final damage has been expressed as a percentage of the total number of rocks in the measurement area with criteria based on the British Standards 6349 seen in table 8:

Table 8: Recommended criteria for rock armour movement (British)

Classification	
0	No discernible movement
R	Rocks seen to be rocking but not permanently displaced
1	Rocks displaced by up to 0.5Dn (<0.5D_n)
2	Rocks displaced by more than 0.5D_n and up to 1.0D_n (0.5-1.0 D_n)
3	Rocks displaced by more than 1.0D_n (>1.0 D_n)

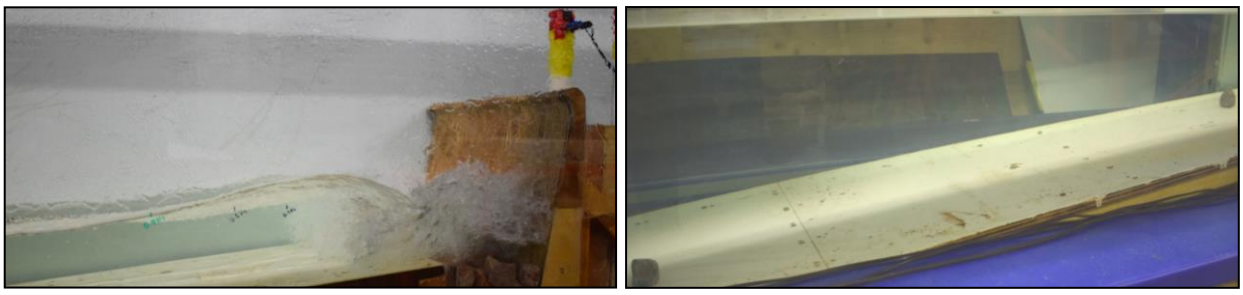

Figure 31: Rock armour displacement down foreshore ramp for 0.7Hz wave

It was noted that the greatest displacement of rock armour, classification 3, was at the largest water level with the largest waves, due to the impulsive loading on the face of the structure however this only occurred for the 0.7Hz waves as these waves broke directly onto the toe as seen in figure 42. Overall, the rock armour was stable with a 'damage percentage' less than 5%.

With preliminary physical modelling conducted by HR Wallingford on the HPC seawall at a reduced scale and with oblique waves involved, a similar damage level was observed and can be seen in Figure 32.

Experimental Limitations and Sources of error

During the testing period it became evident that aspects of the model deviated from the prototype and with hindsight, areas of the experiment could have been improved. Besides the prior effects that occur when conducting physical modelling due to the inability to fulfil perfect similitude, errors can be categorised in the form of systematic, human or random.

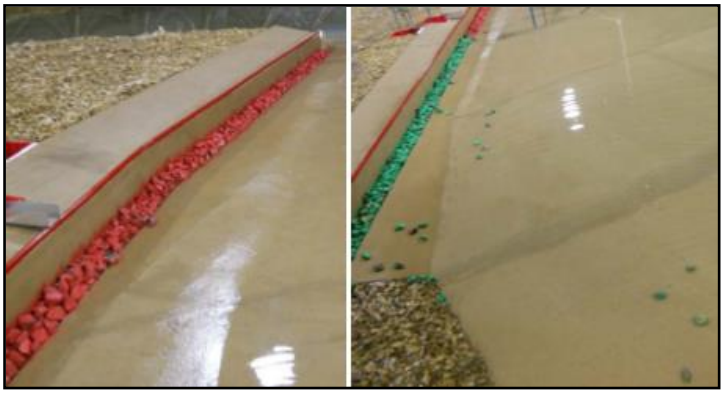

Figure 32: HR Wallingford physical model experiment of the Hinkley Point C seawall showing rock damage

Setup and Methodology

Although the overall model was a good representation of the seawall prototype, like most laboratory models and setups, imperfections were present.

Once the model was in the water, it was noticeable that the toe of the ramp had to be held down and this was done with a 20kg weight placed on the toe as seen in Figure 33. This created a source of error as the weight affected the approaching waves through obstruction. This not only affected the reflection of the waves but the profile of the waves and thus the overtopping volumes and distances. It caused the waves to lose some energy and therefore not to travel as far.

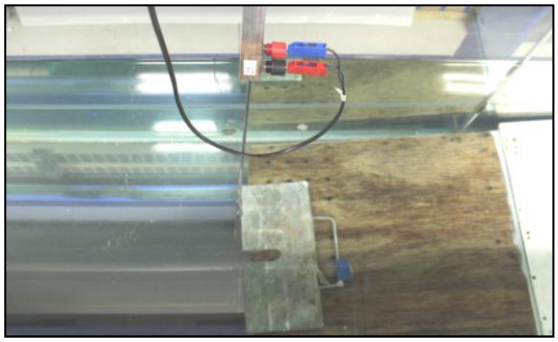

Figure 33: Weight placed on toe of foreshore ramp

The prototype seawall spans alongside the Bristol Channel experiencing oblique waves due to the topography of the area. Testing in the flume, although ideal to measure overtopping rates against wind and analyse the structures performance, it is fundamentally incorrect especially when testing the performance of an idealised structure. It is extremely difficult to reproduce natural waves in order to represent a three-dimensional sea state as a two dimensional process with regular and irregular waves propagating in one direction. However, Hughes (1993) mentions that two-dimensional irregular waves are more amenable to theoretical comparison and provide an interim step towards developing a better understanding of the complexities of three-dimensional analysis.

Model structure

As already discussed, every reasonable effort was made to produce a geometrically accurate and similar scaled model to as large as possible that would still yield valid results. With the marine plywood seawall constructed through the means of gluing, sanding and varnishing offcuts produced from the water jet to model the full effects of the bullnose, there was a high degree of accuracy in terms of the seawall model. Using a dowel to align the offcuts and sanding the structure after, provided a perfect likeliness in terms of geometric shape, roughness and buildability. The model foreshore (Figure 35) was untouched and left as a smooth 8° plywood-constructed slope despite the prototype consisting of an irregular slope with smooth, natural, varying sized boulders (Figure 34).

Figure 34: Hinkley Point C foreshore

Figure 35: Model foreshore with 8° slope

Error was introduced at this point as the slope did not have an equivalent roughness and thus less frictional resistance. This affected the rate of overtopping of the model as waves propagated and “run-up” the slope more easily thus approaching the wall with more energy and subsequently increasing the rate of overtopping – this would overestimate the overtopping volume of the model (Wolters, 2007). It is extremely difficult to quantify this systematic error without the production of a comparable model slope however, it has been assumed that this issue did not substantially affect the rate of overtopping. Furthermore, in specific wave conditions, these boulders in the prototype can build up against the seawall and cover the rock armour. This accumulation will increase the rate of overtopping upon impact however, the use of a smooth foreshore did not allow the opportunity to reproduce and observe this.

The 8° slope has been assessed by surveyors who have conducted a site investigation prior to seawall construction. In practice, the beach level and slope would vary throughout as it is based on the local sediment climate. During testing, it is almost impossible to account for different conditions however an estimated approach bathymetry induces error in terms of wave shoaling and subsequent dissipation – 2 elements affecting overtopping.

Water Level

Three water levels were determined that represented a 1 in 1, 1 in 100 and 1 in 1000 storm event. Using this established and published process provided by the Environmental Agency (EA), accurate water levels accounting for astronomical tide, the local surge shape and extreme sea level were used to formulate a resultant tidal curve.

Although this process provides statistically accurate results, it was based upon many assumptions that could reduce the overall validity. The surge component itself included a rise in sea level pertaining to low pressure weather systems and its associated storm winds however it did not account for local wave setup which can arise near the coastline. For the sake of this experiment, it was deemed that the local wave setup would not have a substantial influence on the overall level. Furthermore, the surge shapes provided by the EA are highly variable between different extreme events however, for practical purposes, it is convenient to have a standard surge shape that is used to generate the resultant tidal curves. Conversely, having a common surge shape for each area causes each event to be standardised which is not possible in nature and reduces variability. Lastly, a significant problem from this process is that it is assumed extreme sea level, peak astronomical tide and peak surge height is coincident in time however in reality, the chance of this occurring is extremely low, but for the purpose of this experiment, it assumes a worst-case scenario which is sufficient when trying to evaluate the design and performance of this coastal structure. These assumptions may not provide the most reliable levels, however in practice a balance needs to be established between accuracy and theoretical calculations to establish an optimum method to generate these water levels.

Slight changes of water levels were experienced overnight in the laboratory due to condensation/evaporation induced by temperature changes. This meant that the water levels in the flume were checked before the start of each day and at various points throughout the day to ensure an accuracy of ±1mm was achieved. This therefore eradicated the possibility of a variation in water level reducing the accuracy of the results. Markings were set at 5 different locations along the flume to ensure that the tank, when emptied/filled, reached a consistent water level from the paddle to the structure. When the water levels were changed, time was allowed for the water to settle before simulating the waves to reduce the effect of any uneven surfaces. Overall the calculated and generated water levels provided an accurate basis for the study at HPC.

Wave conditions

The prototype test duration per run varied between 417s for 0.9Hz and 750s for 0.5Hz which equates to 7 and 13 minutes respectively which is shorter than the typical prototype sampling duration of 20 minutes. A longer test would have provided a better average across the number of random waves impacting the structure and any influences of measuring errors and other side effects will be reduced.

Furthermore, the wave heights and wave periods used, were based of a previously conducted extreme value analysis from EDF but the validity of these results have not been assessed however they were used by HR Wallingford during assessment and thus can be applied here.

Wind

Issues were encountered when scaling and measuring wind speed from the blower. In addition to the highly turbulent wind experienced, the velocity of the flow decreased with increasing distance from the blower outlet. In regards to turbulence, it is questionable as to how wind scales from the prototype to the model. In reality, wind velocity does not ‘fade’ over the structure and is assumed to continue indefinitely. This therefore underestimates the effects of wind within the model structure and is a major problem when testing an idealised situation. This underestimation of wind leads to a reduction in overtopping volumes. The failure to reproduce exact prototype wind direction would have had a significant impact upon the results during comparison however this error was proportionally represented over the full range of results so parametrically the relationship is unaffected.

When experimenting within the laboratory, a problem induced is the use of fresh water as oppose to seawater, which creates the disproportion in density (1000kg/m^3 as oppose to 1025kg/m^3). This is due to the difficulty and impracticality of using seawater in the flume in terms of potential corrosion of the equipment. With wind acting upon fluids of different densities, it was difficult to determine the impacts on the results in terms of overtopping volumes.

The positioning of the fan was based on a trial and error approach through knowledge gained from past literature. It was positioned at 90˚ from the model structure as this was observed to have the optimum effect on the overtopping above

the structure and minimal effect on the incoming waves. Wind speed was measured with an anemometer and the variation in readings was observed based on the anemometer position - 2 positions were tested with results varying up to 25%. Despite, the fan angled at an “optimum” position, as the wind speed increased, the higher velocity caused adverse small ripple waves on the surface of the water as observed in figure 36. This affected how the waves interacted with the seawall and the side of the flume.

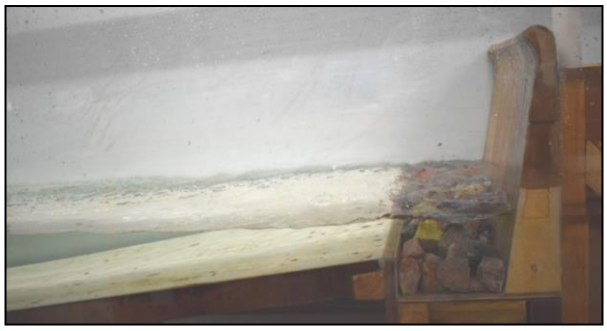

Figure 36: Ripples forming prior to wave run

Collection of Overtopping Volume

Collection buckets were specifically made to collect overtopped discharge. A decision was made for the buckets not too span the full width of the flume to reduce the effect of reflection and friction from the sidewalls in turn reducing this model effect. It was a controversial decision, however a similar concept was adapted by Lioutas, Smith and Verhagen (2012) and this helped validate this idea as this experiment was deemed to provide successful results. However, it was observed that for the larger waves and higher wind speeds, water splashes were distributed more widely and not all captured in the overtopping tanks. This volume was observed to be fairly substantial at times and further increased, proportional to wind speed. It can be thought that this loss would have produced a significant underestimation of the overtopping volume however cannot be quantified.

Figure 37: Gaps between collection buckets

Figure 38: Duct tape applied to reduce water loss

The use of the separate buckets resulted in gaps between the boxes and the structure itself through which the water could have escaped. This problem was noticed prior to testing and duct tape (Figure 38) was applied to the edges to reduce the gap and prevent water being lost. Potentially one unit could have been used and split into individual sectors to reduce gaps.

Despite applying slanted edges to the boxes to prevent water remaining on the edges of the boxes it was noticed at the end of each run, not all water was in the bucket - these droplets were not sufficient to alter the volume. It was observed that large amounts of water had escaped collection especially during the lower frequency waves at the higher water levels despite numerous attempts at trying to reduce the amount of water leaving the tank and escaping collection.

Figure 39: Water escaping the collection buckets at the higher wind speeds

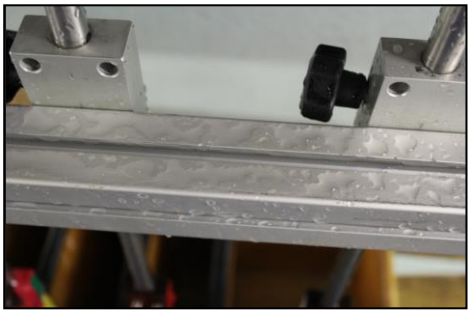

Figure 40: Water remaining on the edges of the wave probe brackets

In-situ wave gauges had initially been planned to measure the overtopped volume in each bucket however unfortunately it was not possible to obtain a reading despite preliminary testing. It was believed to be due to oxidation of the copper strip caused by the minute changes in temperature however, that was a factor unable to be controlled or measured. The alternative was to use wave probes which provided accurate readings however were a source of obstruction to incoming waves in turn reducing the overtopped volume but again, at the end of the run, drops were observed but would not have increased the discharge. A temporary sheet could have been installed to stop this water and direct it into the bucket however introduces a major model effect.

Materials

Wood had to be used for model construction due to the availability of materials, which was convenient for scaling however if the experiment could be repeated, a lightweight metal would be ideal to eliminate some of the wood limitations such as

buoyancy and warping. This buoyancy effect caused the beach to lift up at times causing inconsistent wave propagation and breaking effects between the spectra. A more dense material would have been best to prevent this but this effect occurred on the last few runs - the beach performed well up until this point despite securing it with silicone sealant.

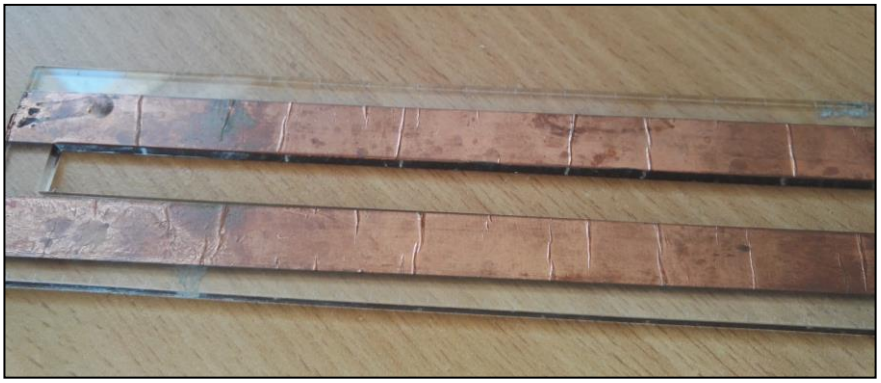

Figure 41: Potential oxidation to the wave gauges

Further Testing and Recommendations

Wind generated effect on overtopping is a topic of research that has been carried out before however never on the Hinkley Point C seawall which made background research extremely difficult and therefore there are still opportunities for research in this subject. Areas of this experiment have adapted previous methods in an aim to improve the accuracy and ease of physical modelling.

As mentioned earlier, when modelling an idealised structure like this, the need to construct the whole wall as oppose to only a section is a necessity as it provides the opportunity to analyse and visualise how the whole structure responds when faced with impulsive wave conditions. Modelling the whole section of the wall allows for the testing of oblique waves – a major factor neglected in this experiment. Understandably, it is expected to see some decrease in the ability to generate perfect oblique waves due to the finite restrictions of the laboratory. Despite the ability to replicate physical parameters such as wind, these experiments will never become replicas of the real ocean (Ploeg and Funke, 1985). Nonetheless, should be attempted in the COAST basin. The model will have to be central to ensure edge effects do not have an influence and although a smaller scale will have to be applied due to geometrical restrictions, on balance, it would allow a more accurate representation and conclusion of the structural performance.

Due to availability restraints, if the basin cannot be used, a larger scale model should be tested in a larger flume providing a more accurate depiction of the prototypes wave conditions. With a lack of time, only 7 wind speeds were tested but ideally, a wider range of wind speeds should be tested to provide a conclusive result on the

effects of wind on the rate of overtopping and to further investigate the exponential relationship. More irregular conditions alongside more water levels should also be tested as these are more realistic of the actual sea state and provide a stronger validation of the structures performance. However if regular waves are used, a larger number of waves should be run. 75 waves were chosen in this case due to lack of time and to ensure the collection buckets did not exceed their capacity before the end of the test. More waves do however provide a more representative approach.

In regards to generation and measurement techniques, generating wind speed is an area to be dwelled upon, incorporating the way the wind itself passed over the structure. Ward et al. (1997) detailed how a more consistent flow velocity could be achieved by 'drawing' the wind as oppose to 'blowing' it. The Wind Tunnel Honeycomb could be deployed which aims to reduce turbulence in the form of little tubes thus increasing the accuracy and consistency of measurements reducing the effects of turbulence as mentioned by Hughes (1993). Secondly, measuring the actual overtopping volume is an area to be developed, even though attempted in this study. A new solution or similar idea should be worked upon so that the measuring equipment does not provide any obstruction to overtopping whilst still producing accurate and fast in-situ results.

Conclusion

A physical model of the Hinkley Point C seawall was constructed, tested and analysed in terms of competence of design and compliance of structural performance against a series of regular and irregular waves at 3 different water levels. Investigations were carried out to provide an insight into the relationship between wind and overtopping rate – a study where limited research exists.

Using Froude scaling, the model and wave conditions were scaled accordingly. Seven incremental wind speeds were tested, and it was concluded that the overtopping volume increased with an increase in wind however began to plateaux at a 15 - 17.5m/s prototype speed. The 0.5Hz, 0.6Hz, and 0.7Hz waves produced the greatest overtopping rate with increasing wind speed. These waves broke near or on the toe of the structure, interacting with the rock armour and creating an uprush of aerated water which was directed over the structure with the effect of wind. On average, the lower frequency waves produced an overtopping rate that was 3.5 times greater than the higher frequency waves. Although these results show significant trends, the use of regular waves to model idealised structures are not commonly used especially when aiming to assess the structural performance.

Designers have recommended an overtopping rate limited to 0.1l/s/m for safety and to avoid excessive erosion on the leeward side of the wall. This overtopping rate was exceeded for the lower frequency waves and irregular conditions when the wind speed reached roughly 14.5m/s and hence the structure failed in terms of its primary purpose. To provide a more conclusive result, testing should be carried out in a

coastal basin so oblique waves can be experimented and more conditions should be used at a wider range of wind speeds to determine a more accurate relationship.

Calculating the overtopping rate is a complicated process in which parameters need to be known and understood and physical modelling provides the opportunity to evaluate the parameters that affect design. Physical models provide both qualitative and quantitative information helping understand complex processes such as impact loading/wave breaking which have become more apparent as to what can be expected at HPC and necessary requirements can be taken to improve the structure and positioning of rock armour. These forces are vital as they can cause severe detrimental effects posing problematic situations for contractors and designers.

Overtopping at Hinkley Point C is a new area of research. The lack of knowledge on the area, structure and processes that occur at this type of structure meant that physical modelling was the most effective method to visualise how overtopping was affected by onshore wind speed and the effects of spatial distribution. Existing models placed in the wave flume had yielded strong parametric results but were hindered by a lack of wind speed variability (Ward et al., 1998), and this experiment helped fill the gap. Despite yielding significant results, this topic still requires a more critical approach with improvements, but this study has provided a strong foundation for future students and the industry.

Acknowledgements

I would like to thank Martyn Hann for providing not only his guidance on a suitable topic of research and supervising the project but also continual support throughout a very challenging year. Thanks must go to the technicians: Andrew Oxenham and Gregory Nash in the COAST laboratory for their assistance and expertise during the experimental phase of this project. Bernard Butler should kindly be thanked in regards to monetarily funding for the project. Furthermore, my working partner, Byron Ottey should be thanked for his assistance in completing the physical modelling and prior requirements. On a more personal level, a special mention must go to KierBAM, my friends, family and colleagues for their patience, guidance and encouragement throughout this academic year.

References

(www.geodata.soton.ac.uk), G. (2007). *Channel Coastal Observatory - Seawalls*. [online] Channelcoast.org. Available at: http://www.channelcoast.org/southeast/programme_design/defence_type/?link=seawalls.html [Accessed 6 Sep. 2017].

Allsop, W., Bruce, T., Pearson, J. and Besley, P. (2005). Wave overtopping at vertical and steep seawalls. *Proceedings of the Institution of Civil Engineers - Maritime Engineering*, 158(3), pp.103-114.

Besley, P., Stewart, T. and Allsop, N. (1998). Overtopping of vertical structures: new prediction methods to account for shallow water conditions. [online] Available at: https://www.researchgate.net/publication/290302706 Overtopping of vertical structures new prediction methods to account for shallow water conditions [Accessed 30 Sep. 2017].

Bijlsma,L.,Ehler, C.N.,Klein,R.J.T.,Kulshrestha,S.M.,McLean,R.F., Mimura, N., Nicholls, R.J., Nurse, L.A., Perez Nieto, H., Stakhiv, E.Z., Turner, R.K., Warrick, R.A., 1996. Coastal zones and small islands. In: Watson, R.T., Zinyowera, M.C., Moss, R.H., Impacts, Adaptations and Mitigation of Climate Change: Scienti"c-Technical Analyses. Cambridge University Press, Cambridge, pp. 289}324.

Bird, E. (1996). Beach management. Chichester: John Wiley

Blanco, M., Moreno-Torres, P., Lafoz, M. and Ramírez, D. (2015). Design Parameter Analysis of Point Absorber WEC via an Evolutionary-Algorithm-Based. *Energies*, 8(10), pp.11203-11233.

British Standards Institution, 2003. *BS 6349 – 1 Part 1: Code of practice for general criteria, London*

Bruce, T., Franco, L., Allsop, W. and Pearson, J. (2002). HAZARDS AT COAST AND HARBOUR SEAWALLS –VELOCITIES AND TRAJECTORIES OF VIOLENT OVERTOPPING JET. *ICCE*.

Bruce, T., Pullen, T., Allsop, W. and Pearson, J. (2005). How far back from a seawall is safe? Spatial distributions of wave overtopping. *International Conference on Coastlines, structures and breakwaters*.

Bullock, G., Crawford, A., Hewson, P., Walkden, M. and Bird, P. (2001). The influence of air and scale on wave impact pressures. *Coastal Engineering*, 42(4), pp.291-312.

Burcharth, H. F., & Andersen, T. L. (2009). Scale Effects Related to Small Physical Modelling of Overtopping of Rubble Mound Breakwaters, *Coastal Structures* 2007: Proceedings of the 5th International Conference (pp. 1532-1541). World Scientific Publishing Co

Chanson,H. (2009).Turbulent air-water flows in hydraulic structures: Dynamic similarity and scale effects, Environ. Fluid Mech. 9(2), 125–142.

Chebana, F. and Ouarda, T. (2011). Multivariate quantiles in hydrological frequency analysis. *Environmetrics*, 22(1), pp.63-78.

Church, J. and White, N. (2006). A 20th century acceleration in global sea-level rise. *Geophysical Research Letters*, 33(1), p.n/a-n/a.

CIRIA, CUR, CETMEF (2007). The Rock Manual. The use of rock in hydraulic engineering (2nd edition). C683, CIRIA, London

De Rouck, J., Geeraerts, J., Troch, P., Kortenhaus, A., Pullen, T. and Franco, L. (2005). New Results on Scale Effects for Wave Overtopping at Coastal Structures. *International Conference on Coastlines, structures and breakwaters*. [online] Available at: http://www.icevirtuallibrary.com/doi/full/10.1680/csab2005hsad.34556.0003 [Accessed 28 Oct. 2017].

De Waal J.P., Tönjes P. and van der Meer J., 1996, Wave overtopping of vertical structures including wind effect, *Proceedings of the 25th Int. conf. on Coastal Engineering*, ASCE, 2216-2229.

Douglass S.L. (1984) Irregular wave overtopping rates. *Proc. 19th ICCE, Houston, pp 316-327, ASCE, New York*

Environment Agency. (2011). Coastal flood boundary conditions for UK mainland and islands

EurOtop, 2007. European Overtopping Manual - Wave overtopping of sea defences and related structures: Assessment manual. Van der Meer, J.W., Allsop, N.W.H., Bruce, T., J., Kortenhaus, A., Pullen, T., Schüttrumpf, H., www.overtopping-manual.com.

EurOtop, 2016. Manual on wave overtopping of sea defences and related structures. An overtopping manual largely based on European research, but for worldwide application. Van der Meer, J.W., Allsop, N.W.H., Bruce, T., De Rouck, J., Kortenhaus, A., Pullen, T., Schüttrumpf, H., Troch, P. and Zanuttigh, B., www.overtopping-manual.com.

Exploring our Oceans. (2017). *Amphidromic Points: tidal spiders in a real World*. [online] Available at: http://moocs.southampton.ac.uk/oceans/2014/11/09/amphidromic-points-tidal-spiders-in-a-real-world/ [Accessed 20 Oct. 2017].

French, P. (2004). *Coastal defences*. London: Routledge.

Geeraerts, J., Troch, P., De Rouck, J., Verhaeghe, H. and Bouma, J. (2006). Wave overtopping at coastal structures: prediction tools and related hazard analysis. *Journal of Cleaner Production*, 15(16), pp.1514-1521.

Gōda. Y, (2010), *Random seas and design of maritime structures*, Singapore: World Scientific.

Gommes, R., du Guerny, J., Nachtergaele, F., Brinkman, R., 1997. Potential impacts of sea-level rise on populations and agriculture, FAO, Rome.

Hamill, L. (2001). Understanding Hydraulics, 2nd edition. Palgrave, Basingstoke, England.

Hann, Martyn. (2018). *Chapter 3 – Physical modelling of Coastal Structures*. University of Plymouth, 17th April 2018

Hansen, A., Laugesen, R., Bredmose, H., Mikkelsen, R. and Psichogios, N. (2014). Small scale experimental study of the dynamic response of a tension leg platform wind turbine. *Journal of Renewable and Sustainable Energy*, 6(5), p.053108.

Heller, V. (2011). Scale effects in physical hydraulic engineering models. *Journal of Hydraulic Research*, 49(3), pp.293-306.

Herbert, D. (1996). The overtopping of seawalls - A comparison between prototype and physical model data. *H.R Wallingford*.

HR Wallingford (2000) 'The joint probability of waves and water levels: JOIN-SEA - A rigorous but practical new approach' HR Wallingford Report TR 71

Hudson, R. Y., Herrmann, F. A., Sager, R. A., Whalin, R. W., Chatham, C. E. and Hales, L. Z. 1979. "Coastal Hydraulic models," Special Report No. 5, US Army Engineer Waterways Experiment Station, Vicksburg Mississippi

Hughes, S. (1993). *Physical models and laboratory techniques in coastal engineering.* 7th ed. World Scientific, pp.6-8.

Hunt, A. (2003). Extreme Waves, Overtopping and Flooding at Sea Defences.

Iglesias, Gregorio. (2017). *Chapter 2 - waves*. University of Plymouth, 18th November 2017

Iwagaki, Y., Tsuchiya, Y. and Inoue, M. (1966). On the effect of wind on Wave overtopping on vertical seawalls. *Kyoto University Research Information Repository*.

Jones, D., Zou, Q. and Reeve, D. (2011). MODELLING STORM SURGE WAVE OVERTOPPING OF SEAWALLS WITH NEGATIVE FREEBOARD. *Coastal Engineering Proceedings*, 1(32), p.52.

Juhl, J. and Sloth, P. (1994). Wave Overtopping of Breakwaters under Oblique Waves. *Overtopping under oblique waves*. [online] Available at: http://ascelibrary.org [Accessed 24 Oct. 2017].

Kato, F., Suwa, Y., Watanabe, K. and Hatogai, S. (2012). Mechanisms of coastal dike failure induced by the Great East Japan Earthquake Tsunami. *Coastal Engineering Proceedings*, 1(33), p.40.

Kortenhaus, A., van der Meer, J., Burcharth, H., Geeraerts, J., Pullen, T., Ingram, D. and Troch, P. (2005). Quantification of Measurement Errors, Model and Scale Effects Related to Wave Overtopping.

Le Mehaute, B. 1976. "Similitude in Coastal Engineering," Journal of the Waterway, Harbors and Coastal Engineering Division, American Society of Civil Engineers, Vol WW3, pp 317-335.

Lioutas, A., Smith, G. and Verhagen, H. (2012). SPATIAL DISTRIBUTION OF OVERTOPPING. *Coastal Engineering Proceedings*, 1(33), p.63.

Lorke, S., Brüning, A., Van der Meer, J., Schüttrumpf, H., Bornschein, A., Gilli, S., Pohl, R., Spano, M., Říha, J., Werk, S. and Schlütter, F. (2011). ON THE EFFECT OF CURRENT ON WAVE RUN-UP AND WAVE OVERTOPPING. *Coastal Engineering Proceedings*, 1(32), p.13.

Lundgren, H. 1969. "Wave Shock Forces: An analysis of Deformations and Forcers in the Wave and in the Foundation," *Proceedings of the Symposium on Research on Wave Action,* Delft Hydraulics Laboratory, Emmeloord, The Netherlands, Vol II, Paper 4

Miles, Jon. (2017). *Chapter 6 – Physical modelling*. University of Plymouth, 16th October 2017

Müller, G., Allsop, W., Bruce, T., Kortenhaus, A., Pearce, A. and Sutherland, J. (2008). The occurrence and effects of wave impacts. *Proceedings of the Institution of Civil Engineers - Maritime Engineering*, 160(4), pp.167-173.

National Audit Office. (2017). Hinkley Point C. *Department for Business, Energy & Industrial Strategy*.

Nationalgeographic.com. (2017). *Coastlines*. [online] Available at: https://www.nationalgeographic.com/science/earth/surface-of-the-earth/coastlines/ [Accessed 6 Oct. 2017].

Nature.com. (2017). *Modelling Sea Level Rise | Learn Science at Scitable.* [online] Available at: http://www.nature.com/scitable/knowledge/library/modeling-sea-level-rise-25857988 [Accessed 17 Oct. 2017].

Neill, S., Litt, E., Couch, S. and Davies, A. (2009). The impact of tidal stream turbines on large-scale sediment dynamics. *Renewable Energy*, 34(12), pp.2803-2812.

Neumann, B., Vafeidis, A., Zimmermann, J. and Nicholls, R. (2015). Future Coastal Population Growth and Exposure to Sea-Level Rise and Coastal Flooding - A Global Assessment. *PLOS ONE*, 10(3), p.e0118571.

Peng, Z. and Zou, Q. (2011). Spatial distribution of wave overtopping water behind coastal structures. *Coastal Engineering*, 58(6), pp.489-498. Phillips, M. and Crisp, S. (2010). Sea level trends and NAO influences: The Bristol Channel/Severn Estuary. *Global and Planetary Change*, 73(3-4), pp.211-218.

Ploeg, J., and Funke, E. R. 1985. "The generation of Laboratory Waves: A tool for the Understanding of Wave Dynamics," *Proceedings of International Symposium on Water Wave Research*, SFB 205, University of Hannover, Germany, pp 265-283

Pullen, T., Allsop, W., Bruce, T. and Pearson, J. (2009). Field and laboratory measurements of mean overtopping discharges and spatial distributions at vertical seawalls. *Coastal Engineering*, 56(2), pp.121-140.

Reeve, D., Chadwick, A. and Fleming, C. (2014). *Coastal Engineering: Processes, Theory and Design Practice*. 2nd ed. Spon Press, pp.1-15.

Reis, M., Hedges, T., Williams, A. and Keating, K. (2006). Specifying seawall crest levels using a probabilistic method. *Proceedings of the Institution of Civil Engineers - Maritime Engineering*, 159(4), pp.137-145.

Reis, M., Neves, M. and Hedges, T. (2008). Investigating the Lengths of Scale Model Tests to Determine Mean Wave Overtopping Discharges. *Coastal Engineering Journal*, 50(4), pp.441-462.

Revolvy, L. (2017). *"Hinkley Point C nuclear power station" on Revolvy.com*. [online] Revolvy.com. Available at: https://www.revolvy.com/main/index.php?s=Hinkley%20Point%20C%20nuclear%20power%20station&item_type=topic [Accessed 30 Oct. 2017].

Sakakiyama, T., Kajima, R., Imai, S., Shimizu, T. and Katayama, H. (1996). Field survey of wave overtopping on seawall covered with armor units. *PROCEEDINGS OF CIVIL ENGINEERING IN THE OCEAN*, 12, pp.291-296.

Sartini, L., Mentaschi, L. and Besio, G. (2015). Comparing different extreme wave analysis models for wave climate assessment along the Italian coast. *Coastal Engineering*, 100, pp.37-47.

Southwalesports.co.uk. (2017). *Bristol Channel Tides - ABP South Wales*. [online] Available at: http://www.southwalesports.co.uk/Marine_Information/Marine_Information/Bristol_Channel_Tides/ [Accessed 9 Oct. 2017].

Sunamura, T. and Okazaki, S. (1996). Breaker Types and Wave Reflection Coefficient: Laboratory Relationships. *Journal of Coastal Research*, 12(1), pp.240-245.

Surgewatch.org. (2017). *Tidal range | SurgeWatch*. [online] Available at: https://www.surgewatch.org/definition/tidal-range/ [Accessed 9 Oct. 2017].

Suzuki, T., Tanaka, M. and Okayasu, A. (2003). Laboratory experiments on wave overtopping over smooth and stepped gentle slope seawalls. *Asian and Pacific Coasts.*

ThoughtCo. (2017). *All You Wanted to Know About Ocean Waves*. [online] Available at: https://www.thoughtco.com/what-are-waves-1435368 [Accessed 9 Oct. 2017].

TIDE TABLE 1B - UK AND IRELAND. (2017). [S.l.]: U K HYDROGRAPHIC OFFICE.

Van der Meer, J., Pullen, T., Allsop, W., Bruce, T., Schüttrumpf, H., and Kortenhaus, A., (2009) Prediction of Overtopping. Handbook of Coastal and Ocean Engineering: pp. 341-382

van Rijn, L. (2018). Stability Design of Coastal Structures. *Stability of coastal structures*.

Visitmyharbour.com. (2017). *Spring and Neap tides, explanations and example by VisitMyHarbour [Tide] - VisitMyHarbour articles*. [online] Available at: http://www.visitmyharbour.com/articles/3154/spring-and-neap-tides-explanations-and-example [Accessed 29 Oct. 2017].

Ward, D. (1998). *Wind effects on runup and overtopping of coastal structures*.

Ward, D., Wibner, C. and Zhang, J. (1997). Advection Distance of Water Droplets in Strong Winds. *Journal of Waterway, Port, Coastal, and Ocean Engineering*, 123(5), pp.297-299.

Weller, S., Stallard, T. and Stansby, P. (2010). Experimental measurements of irregular wave interaction factors in closely spaced arrays. *IET Renewable Power Generation*, 4(6), p.628.

Wolters, G. and R.A. van Gent, M. (2007). Maximum wind effect on wave overtopping of sloped coastal structures with crest elements. [online] Available at: https://www.researchgate.net/publication/259259050_MAXIMUM_WIND_EFFECT_ON_WAVE_OVERTOPPING_OF_SLOPED_COASTAL_STRUCTURES_WITH_CREST_ELEMENTS [Accessed 6 Sep. 2017].

www4.edesign.co.uk. (2018). *Wave Gauges* | *Edinburgh Designs*. [online] Available at: http://www4.edesign.co.uk/product/wavegauges/ [Accessed 9 Feb. 2018].

Xu, Z., and A. J. Bowen, 1994: Wave- and wind-driven flow in water of finite depth. J. Phys. Oceanogr., 24, 1850–1866.

Appendices are available as ‘supplementary files’ (please see download area)